



OPEN

Assessment of groundwater potential zones in Kuwait's semi-arid region: a hybrid approach of multi-criteria decision making, Google earth engine, and geospatial techniques

Mohamed A. Atalla¹, Ali Shebl^{2,3}✉, Bojan Đurin⁴, Nikola Kranjčić⁵✉ & Wael M. AlMetwaly⁶

Recently, the use and management of water resources have become a critical issue, especially in arid and semi-arid surroundings. In such areas, the importance of mapping groundwater potential zones is unmeasurable since water is a critical human resource. Focused on the semi-arid region of Kuwait, our research integrates Google Earth Engine and multi-criteria decision-making (MCDM), offering a robust admission to identifying groundwater potential zones. To this end, thirteen criteria including geology, slope, rainfall, elevation, Normalized Difference Vegetation Index (NDVI), Normalized Difference Water Index (NDWI), Land Surface Temperature (LST), drainage density, Land Use and Land Cover (LULC), lineament density, topographic wetness index (TWI), geomorphology, and the water table were integrated to reach a wise decision through AHP-MCDM. Our findings revealed that Kuwait's groundwater potential zones are extremely well suited to the country's north and east. Appropriate potential zones with high and moderate degrees encompass 12% and 37%, respectively, while extremely high suitability is less than 1.5%. These findings are based on the input data (mainly rainfall, NDVI, NDWI, and LST). The likelihood of groundwater potential is higher in the lower regions of the country. Over 7500 km²—nearly 50% of the total area—are classified as low potential. Furthermore, Our research shows that combining more factors can increase precision while ensuring the stability of the detection process of GWPZs. Around 242 km² as promising targets for future groundwater exploitation within Kuwait. Rigorously validated through on-site field observations and corroborated by maps showing the distribution of productive groundwater wells in Kuwait, our results exhibit a considered alignment. It is recommended that we extend the application of our methodology beyond the borders of the studied terrain and urge decision-makers to consider our findings in their strategic planning processes.

Keywords Semi-arid region, Groundwater potential, Google Earth Engine, Multicriteria decision, Kuwait

Groundwater is an essential lifeline for various purposes, especially in arid and semi-arid regions¹. Kuwait faces persistent water resource shortages and water quality issues in an arid region. Kuwait faces one of the highest per capita consumption rates in the world. The country grapples with acute water scarcity, leading to significant annual expenses on direct water supply and distribution². Kuwait's renewable water resources per person have

¹Department of Geography, and Survey, Higher Institute for Literary Studies in King Mariout, Alexandria, Egypt.

²Department of Mineralogy and Geology, University of Debrecen, Debrecen 4032, Hungary. ³Department of Geology, Tanta University, Tanta 31527, Egypt. ⁴Department of Civil Engineering, University North, Varaždin 42000, Croatia. ⁵Department of Geodesy and Geomatics, University North, Varaždin 42000, Croatia. ⁶Department of Geography and GIS, Faculty of African postgraduate Studies, Cairo University, Giza 12613, Egypt. ✉email: alishebl@mailbox.unideb.hu; nkranjcic@unin.hr

experienced a gradual decline, decreasing from 17.3 m³/year in 1977 to 4.8 m³/year in 2018². As a result of this scarcity, the country heavily depends on desalination plants to manage its freshwater requirements.

The availability of usable groundwater in Kuwait is limited, with the water mostly being brackish to salty. Unfortunately, even these available scarce fresh groundwater lenses are at risk due to mismanagement (excessive pumping), leading to a decline in water quality (salinity deterioration) through excessive pumping³. An example can be found in Al-Rawdatain and Umm Al-Aish areas, where substantial fresh groundwater reserves provided approximately 20 mm³/year during the early 1960s. However, recent mismanagement has significantly reduced this potential to merely 3 mm³/year. Moreover, improper placement of well screens between transition zones of different water bodies or poor design in brackish-saline zones³ can exacerbate salinity issues, negatively affecting Kuwait's water resources. Even brackish groundwater with total dissolved solids (TDS) ranging between 1000 and 10,000 mg/l, which is still considered strategically crucial for Kuwait, has not been spared from the detrimental effects of over-pumping. Salinity levels have surged from 4000 to 20,000 mg/l following excessive pumping activities.

Addressing the depletion of groundwater resources in Kuwait requires effective management of pumping practices, comprehensive plans for groundwater exploration, and the strategic siting of groundwater boreholes based on well-planned studies. Recently, remote sensing and geoinformatics have demonstrated their effectiveness in identifying potential groundwater zones^{4–11}. Additionally, diverse multi-criteria decision-making methods such as regression models¹², frequency ratio¹³, influencing factor¹⁴, and Analytic Hierarchy Process (AHP)^{6,15} have introduced good results regarding groundwater potentiality mapping.

In Table 1; Fig. 1, a literature review is presented. Literature is organized to show which thematic layers different authors used to identify groundwater potential zones in other parts of the world. Based on Fig. 1, it is clear that among 15 studies, all of them used slope in their research. Most of them used land use and land cover (14), lineament density (14), drainage density (13), geology/lithology and rainfall (12), and geomorphology (9). Other thematic layers, such as the digital elevation model, normalized differential vegetation index, and topographic wetness index, are used in a few research studies. Indices such as NDWI, LST study, and DTW are not frequently used, which suggests that our research has a holistic approach toward our aim.

To tackle this pressing issue for Kuwait, the current research endeavors to develop a solution by modeling groundwater potential zones in Kuwait, integrating multiple parameters using Fuzzy-AHP and GIS techniques. The key novelty of this research is that it marks the first comprehensive study to characterize Kuwait's groundwater resources by integrating a wide range of datasets, including geological, hydrological, and climatic information. By employing advanced multicriteria analysis alongside cutting-edge web-based tools such as Google Earth Engine (GEE), this work sets a new precedent in groundwater assessment for the region. The main contribution of the current research is the holistic application of all relevant factors after conducting a comprehensive literature review to build a groundwater potential map for Kuwait as a whole. Additionally, the current study integrates GEE analysis of climatic conditions and various indices with geological, morphological, and hydrogeological factors to provide suitable recommendations for the entire groundwater system in Kuwait. These approaches have shown promising results in offering viable recommendations for water-related challenges in arid and semi-arid surroundings.

Literature review	GL	G	LULC	R	LD	DD	DEM	S	NDVI	NDWI	LST	DTW	TWI
Ibrahim-Bathis and Ahmed ¹⁶	-	+	+	+	+	+	-	+	-	-	-	-	-
Nigussie et al. ¹⁷	-	+	+	+	+	+	+	+	-	-	-	-	+
Abdulkerim et al. ¹⁸	+	-	+	+	+	+	-	+	-	-	-	-	-
Agarwal et al. ¹⁹	+	+	-	-	+	+	-	+	-	-	-	-	-
Abebreste et al. ²⁰	+	+	+	-	+	+	-	+	-	-	-	-	-
Doke et al. ²¹	+	+	+	+	+	-	-	+	-	-	-	-	-
Magesh et al. ²²	+	-	+	+	+	-	-	+	-	-	-	-	-
Senanayake et al. ²³	+	+	+	+	+	+	-	+	-	-	-	-	-
Shebl et al. ⁶	-	-	+	-	+	+	-	+	+	-	-	-	+
Aju et al. ²⁴	+	+	+	+	+	+	+	+	-	-	-	-	-
Hasanuzzaman et al. ²⁵	+	+	+	+	+	+	+	+	+	-	-	-	+
Hagos and Andualem ²⁶	+	-	+	+	-	+	-	+	-	-	-	-	-
Etikala et al. ²⁷	+	+	+	+	+	+	-	+	-	-	-	-	-
Mallick et al. ⁷	+	-	+	+	+	+	+	+	+	-	-	-	+
Ghanim et al. ²⁸	+	-	+	+	+	+	-	+	-	-	-	-	-

Table 1. Literature review of the theme used to identify groundwater potential zones. GL geology and lithology, G geomorphology, LULC land use & land cover, R rainfall, LD lineament density, DD drainage density, S slope, NDVI normalized difference vegetation index, NDWI normalized difference water index, LST land surface temperature, TWI topographic wetness index, DTW depth to water table.

NUMBER OF USED THEMATIC LAYERS

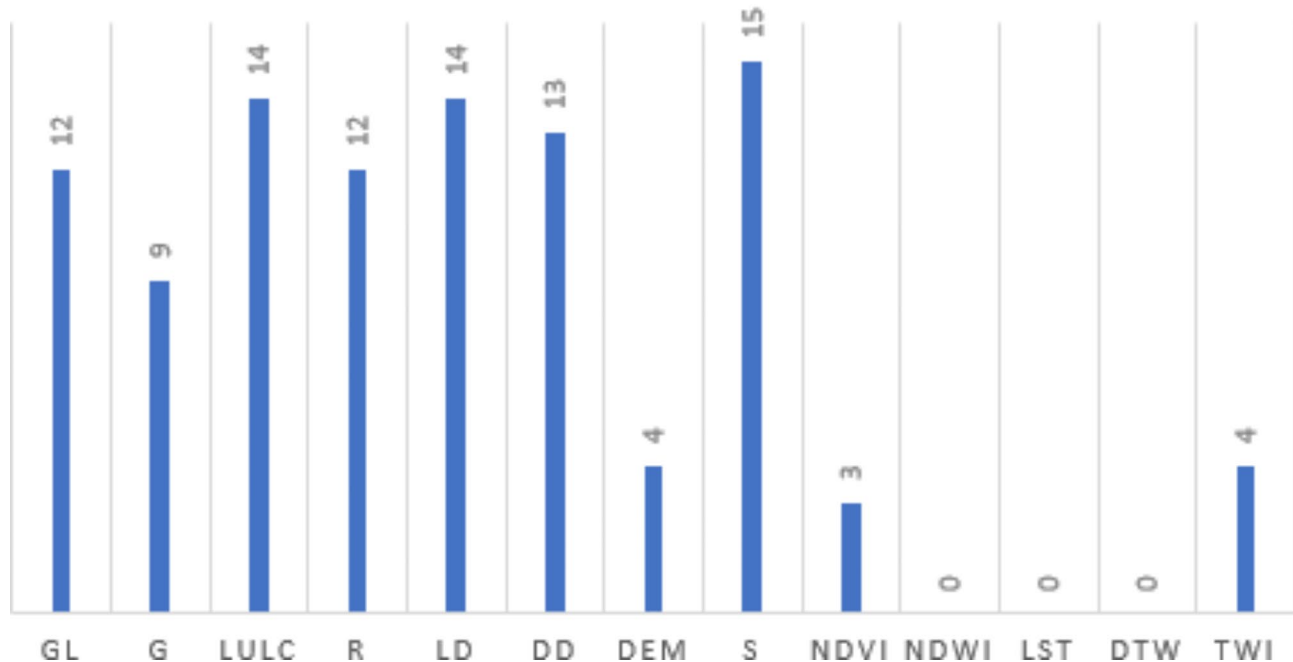


Fig. 1. Overview of the number of thematic layers used in literature. *GL* geology and lithology; *G* geomorphology; *LULC* land use & land cover; *R* rainfall; *LD* lineament density; *DD* drainage density; *S* slope; *NDVI* normalized difference vegetation index; *NDWI* normalized difference water index; *LST* land surface temperature; *TWI* topographic wetness index; *DTW* depth to water table.

Description of the study area

Site description

Kuwait is located in the northwestern part of the Arabian Gulf, situated between latitudes $28^{\circ} 30'$ and $30^{\circ} 05'$ to the north and longitudes $33^{\circ} 46'$ and $30^{\circ} 48'$ to the east Fig. 2. It shares its southern and southwestern borders with Saudi Arabia, while its northwestern border is with Iraq. Kuwait's eastern coastline borders the Arabian Gulf. Figure 1 illustrates that the country includes several islands, where the largest is Bubiyan Island, followed by Warba Island, and the nearest to the coast, Failaka Island. The total land area covers 17,818 km².

Generally, Kuwait's topography is characterized by a mostly flat terrain with a somewhat uneven desert consisting of gently rolling plains covered in gravel. The land gradually inclines from sea level along the eastern coast of the Arabian Gulf towards the west and southwest. Based on Fig. 3A,B. The highest point in the southwestern corner reaches 284 m above sea level. Small hills are scattered across Kuwait, including those along the Jal Al-Zour ridge, which rises to 145 m and overlooks the northern coast of Kuwait Bay. This ridge stretches from the northeast to the southwest, near Jahra. Additionally, there are hills like Al-Laiyah and Keraa Al-Marw, which stand at 138 m in height, and Al-Ahmadi Hill in the southern region of Kuwait, reaching an elevation of 125 m. These hills are more extensive and elongated than the earlier ones, and they are covered with pebbles of various sizes.

Kuwait also features numerous valleys, lowlands locally known as Al-Khubarat, and dunes. Among the notable valleys in Kuwait are the Al-Batin Valley, which runs along the country's western borders, and the Al-Sheqaq Valleys, situated in the northwestern part of the country. Al-Khubarat are distributed in various areas, with the most significant being Al-Rawdatain and Umm Al-Aish, both located in the northern region²⁶. The central geological units covering Kuwait are introduced in Fig. 3C. Figure 3D illustrates the extensive array of geomorphological features covering Kuwait's landscape. These features consist of desert plains and dunes distributed across Kuwait's south and southeastern areas and shaped by the effects of wind, resulting in impressive Aeolian desert formations. The primary geomorphic characteristics include sandy areas (mobile sand sheets), stony surfaces (containing calcrete and gypcrete deposits), minor ridges, and Karst depressions. Additionally, the region encompasses coastal plains and tidal flat features, with the most significant geomorphic elements being recurved spits, sandy beach deposits, silt and clay-based evaporite deposits, and sabkhas. Various igneous and metamorphic rocks also characterize gravel ridges (comprising pebbles and gravel). Inter-ridge surfaces and playa deposits are found across the Fan Delta surface, primarily influenced by the ancient river system along Wadi Al-Batin^{26,27}. Figure 3E shows the general level of the water table within Kuwait, and the distribution of the total dissolved solids is presented in Fig. 3F.

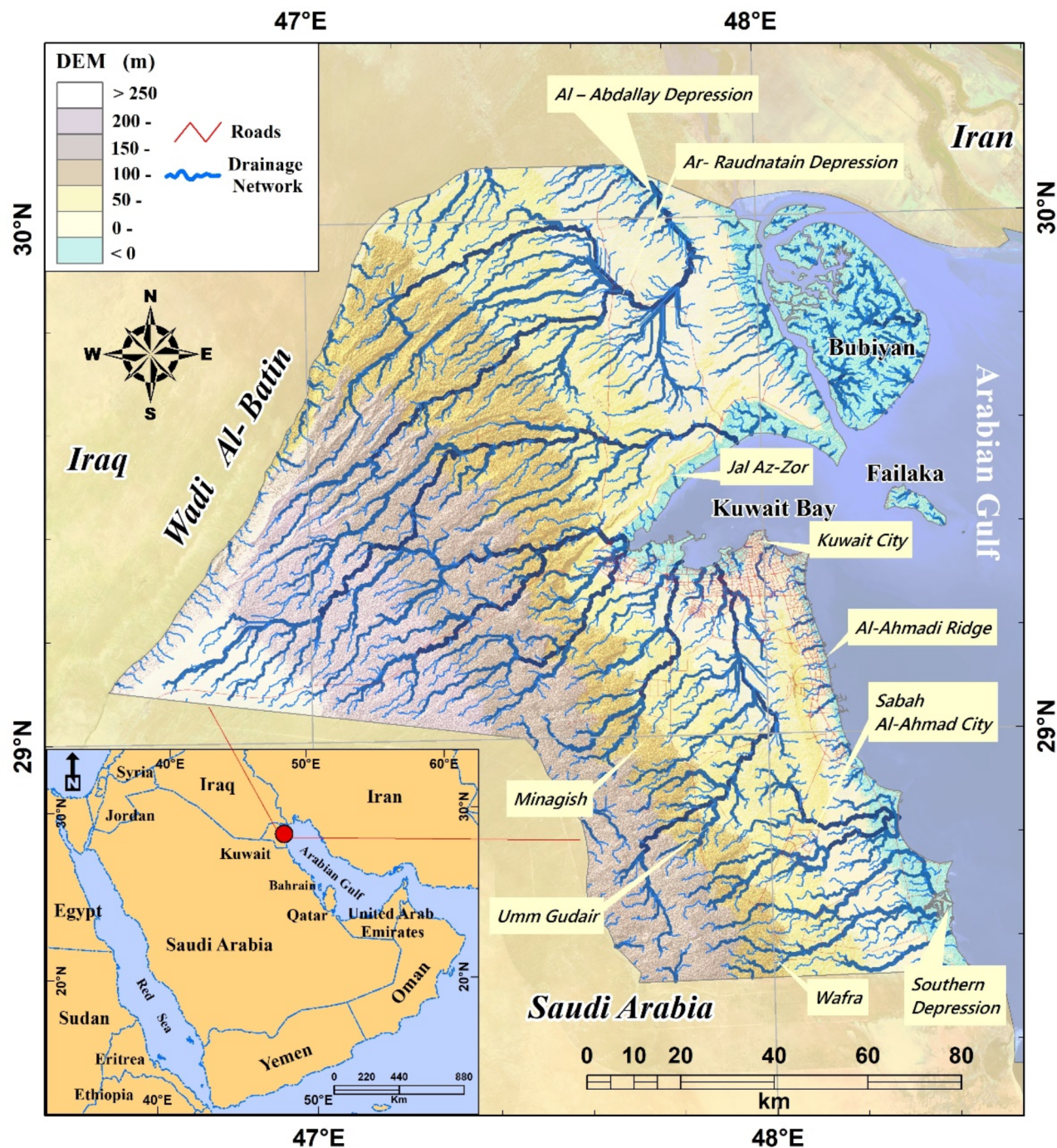


Fig. 2. The study area's location map (Kuwait) shows its main features and the drainage network over the state.

Climatic conditions

The climate of the State of Kuwait is characterized by long, hot, dry summers and short, warm winters with occasional rain. During the summer months, dust-laden winds are common, and humidity in the air increases³². The highest temperature recorded throughout history was 51 °C in July 1978, and the lowest reached –4 °C in January 1964. According to information from the General Directorate of Civil Aviation, average temperatures usually range between 47 °C in summer and 6 °C in winter. These significant temperature differences vary with changes in annual precipitation rates, ranging from 22 mm to 352 mm per year³³. Figure 4A presents average precipitation. The “mean daily maximum” (solid red line) shows the maximum temperature of an average day every month in Kuwait. Likewise, the “mean daily minimum” (solid blue line) shows the average minimum temperature. Hot days and cold nights (dashed red and blue lines) show the average hottest day and coldest night

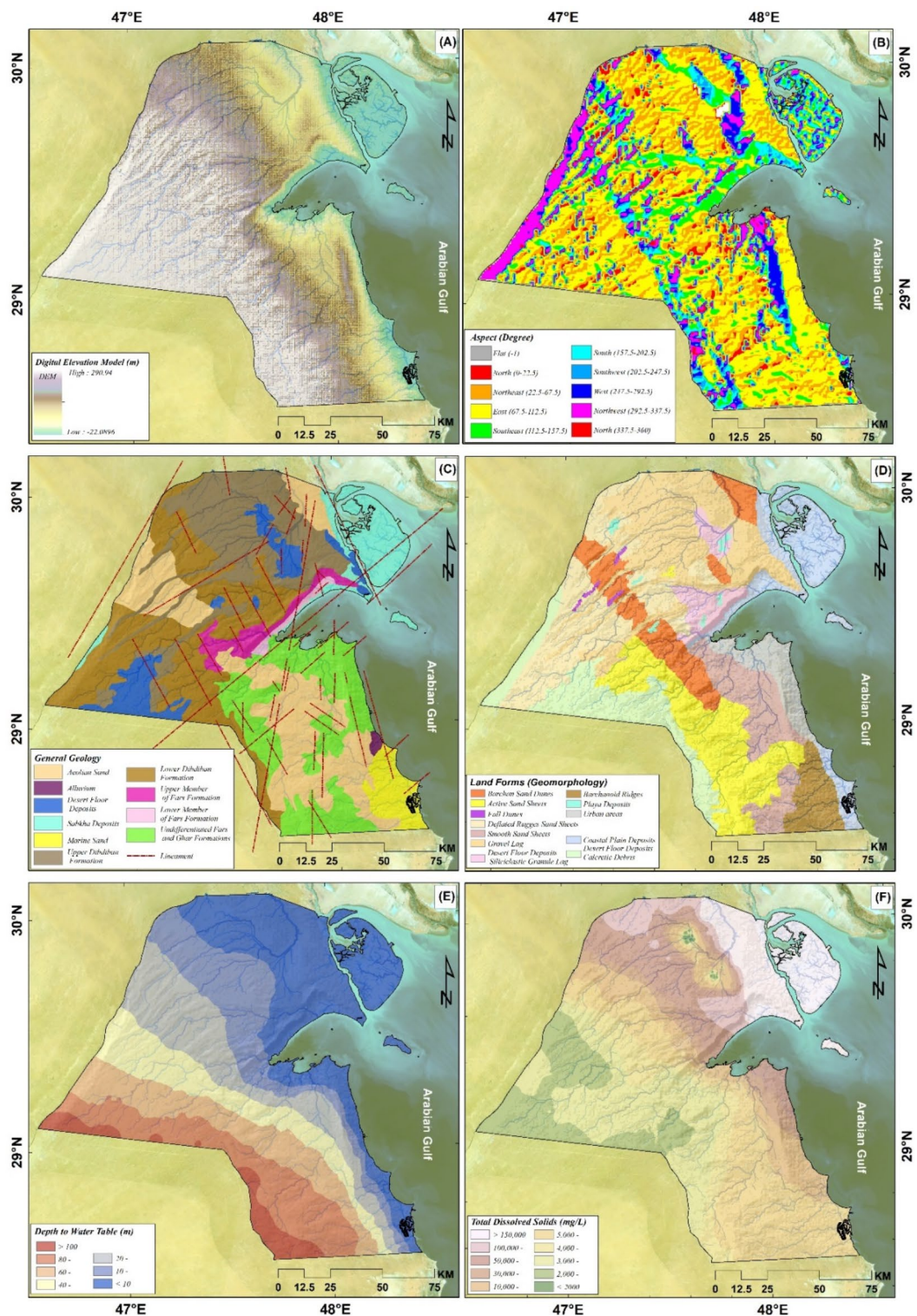


Fig. 3. Research area: (A) Digital elevation model²⁹; (B) Aspect; (C) General geology; (D) Geomorphology³⁰; (E) Depth to water³¹; (F) Total Dissolved solids³¹.

of each month of the last 30 years. Temperatures, and be prepared for hotter and colder days. Wind speeds are not showed per default but can be enabled at the bottom of the graph. Figure 4B presents wind rose in Kuwait.

Geology and hydrogeology

Figure 3C illustrates the exposed rock formations in the study area, originating from sedimentary deposits from the Palaeocene to the recent period. These formations can be categorized into Al-Hasa and Kuwait³⁵. The Al-

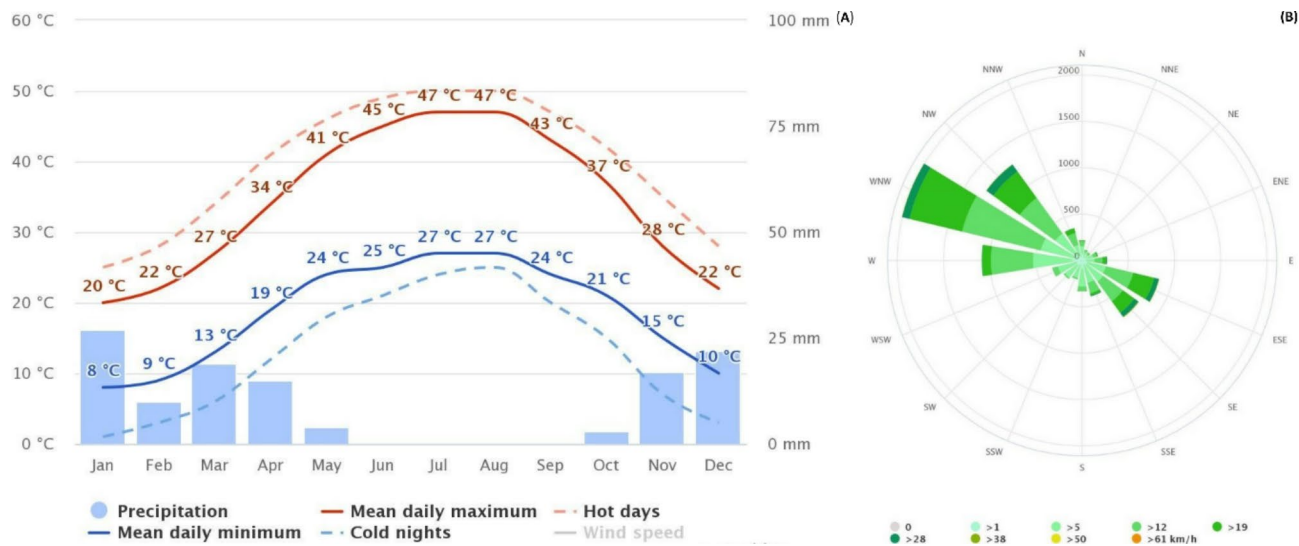


Fig. 4. (A) Average monthly precipitation and temperature for Kuwait; (B) Rose wind³⁴.

Hasa group comprises limestone, dolomite, anhydrite, and clay. It is divided into three formations: Umm er Radhuma from the Palaeocene to the Middle Eocene, Rus in the Lower Eocene, and Damman in the Middle Eocene. The Damman Formation unconformably overlays the Middle Eocene dolomite-limestone of the Dammam Formation. It varies in thickness from 390 m in the northeast to just 8 m in the southeast of Kuwait³⁶.

On the other hand, the Kuwait Group is composed of fluvial sediments such as sand, gravel, calcareous sand, sandstone, clays, gypsum, limestone, and marl. It consists of three formation units, which were formed in Ghar in the Miocene, Fars in the Pliocene, and Dibdibba in the Pleistocene. These formations originated from torrential floods that transported rock formations from the Arabian Peninsula and deposited them in northern Kuwait. The lower member of the Dibdibba Formation is extensively exposed in Kuwait's western and north-central parts, consisting of weathered medium to very coarse-grained calcareous sandstones with grit and pebbles. The upper member of the Dibdibba Formation can be found beneath the undulating plain in the north and northeast Kuwait, extending south-westward southwestward along the characteristic curved ridges of the northwestern area. This upper member consists of a sequence of ungraded, often cross-bedded sands and gravels with occasional intercalations of sandy mud³⁷.

Additionally, the study area includes sedimentary formations from the Quaternary era, specifically the Pleistocene and Holocene. These formations encompass land deposits of gravel and sand and coastal deposits of calcareous sandstone, sand, and mud. The area is characterized by multiple lineaments with various orientations, including N-NE/S-SW, NE/SW, and N-NW/S-SE³⁸. Experience rapid reductions in floodwater flow due to quick infiltration into the dry and porous substrate. In the past, river networks supplied water to the desert, eventually forming groundwater. However, Kuwait's groundwater is considered fossil water due to challenges in replenishing and maintaining it under current climatic conditions. Kuwait has two main groundwater layers. The upper layer, known as the Kuwait Group aquifer, consists of greenish gravelly sands, estimated to be about 7,000–10,000 years old, coinciding with the northward incursion of the summer monsoon in northern Arabia. Intense summer monsoons likely contributed to forming active stream networks in northeastern Arabia and Kuwait, carving the landscape, and forming the Kuwait Group aquifer. The lower layer, known as the Dammam formation, comprises chalky limestone and dolomite. The Kuwait Group Aquifer is unconfined, allowing water to infiltrate from the surface, while the Dammam Formation is confined, with impermeable layers above and below it^{39,40}. As illustrated in Fig. 3E, groundwater flows from higher elevations in the southwest, approximately 90 m above sea level, toward the Gulf Coast in the northeast, consistent with Kuwait's topography. This understanding is supported by hydrogeological studies that confirm the vulnerability of the Kuwait Group to contamination and the salinity issues in the Dammam Formation resulting from over-extraction. Groundwater quality varies from moderately saline in the southwest to highly saline in the northeastern region, as shown in Fig. 3F.

Freshwater lenses are found in the north, such as in Al-Roudtai and Umm Al-Aish. Several geological and rock conditions contributed to their formation, including heavy rainfall exceeding the infiltration capacity into surface depressions, the creation of local surface pools, and the rapid infiltration of accumulated rainwater into the groundwater. These freshwater resources contain less than 1000 mg/L of total dissolved solids and have been used for drinking and bottled water production, with their extraction for drinking purposes ceasing due to the development of desalination plants³¹.

Data used

Elevation

The region's altitude is a basic aspect of its topography and plays a crucial role in evaluating groundwater possibilities. Utilizing elevation data from ALOS PALSAR, we examined the topography of the area, visually depicted in Fig. 3A, B.

Slope

The slope is pivotal in influencing various factors, including surface runoff, groundwater recharge, etc. Steeper slopes hinder groundwater infiltration with regards to the rapid increase in surface runoff during the rainfall and heightened soil erosion rates. Conversely, areas with gentler slopes promote more significant groundwater recharge, allowing rainwater to remain longer and gradually seep into the ground⁶. Consequently, the hill demonstrates an inverse relationship between infiltration rates and surface water infiltration while positively correlating with surface runoff⁴¹. This aspect can prolong the time water infiltrates the soil in areas with gentle flooding, ultimately raising the groundwater Tables^{19,21,42-45}. To determine the surface slope, spatial analysis tools within the ArcGIS environment were employed, utilizing high-precision ALOS PALSAR digital elevation models (DEM) with a 12.5 meters spatial resolution as shown in the Fig. 5A^{46,47}.

Drainage density

Drainage density is of a importance in assessing groundwater movement and recharge as it directly influences the speed of water flow and its ability to penetrate the aquifer. The relationship between drainage density and surface runoff, which subsequently affects water infiltration into the ground, is inversely related to permeability^{5,6,48}. It is vital to identify potential groundwater areas since the drainage density influences the groundwater recharge rate in a specific region. High drainage density areas generally have a lower potential for groundwater recharge due to increased surface runoff rates. Conversely, regions with lower drainage density often exhibit higher groundwater potential as they offer more significant opportunities for groundwater replenishment. ALOS PALSAR DEM data was used to create a drainage network map shown in Fig. 5C, followed by the Line Density spatial analysis tool in ArcGIS to produce a drainage density map^{18,20,21,44,49-51}.

Lineament density

Lineaments play a crucial role in replenishing underground groundwater. They are responsible for enhancing the porosity and permeability of the essential groundwater indicators when rainwater infiltrates the soil. Lineaments also assist in identifying potential groundwater locations. The presence and flow of groundwater depend on the infiltration facilitated by these contours. A higher density of lineaments indicates a more significant potential for groundwater recharge, while a lower density suggests a lower likelihood of finding a potential groundwater source. According to Magowe and Carr^{21,52,53} there is a positive correlation between increased lineament density and potential groundwater areas. To implement this theory, a numerical score was assigned to lineament density. The identification of areas with the greatest groundwater potential was based on their proximity to regions characterized by high lineament density, which were subsequently assigned the highest grades, as demonstrated in Table A (1). Utilizing the “kernel density” method within a Geographic Information System (GIS) framework, a lineament density map was generated to visualize these findings as shown in the Fig. 5D.

Rainfall

Rainfall is indispensable for the hydrological cycle as it serves as the main source of freshwater and directly impacts the replenishment and augmentation of groundwater that percolates into the earth's subsurface layers through fissures and soil or via water flowing through the drainage network, depending on topographical conditions. The region relies on seasonal rainfall received from the northeastern and southwestern monsoons. Researchers have highlighted the crucial role of rainfall density, intensity, and duration in influencing the percolation process. High-intensity, short-duration rainfall leads to reduced percolation and increased surface runoff, whereas low-intensity, long-duration rainfall contributes to a higher percolation rate than surface runoff. Consequently, the quantity of rainfall in the area matters, and the duration and density of rainfall play a crucial role in groundwater recharge. Various researchers have emphasized a strong positive relationship between rainfall and groundwater likelihood, indicating that heavy rainfall suggests a more significant potential for groundwater recharge. Conversely, reduced rainfall has a lower chance of reaching the groundwater^{18,21,43,50}. Rainfall data from the IMERG dataset for the period 2000–2022, obtained from the Precipitation Measurement Missions <https://www.chrsdata.eng.uci.edu>, (PMM) at the University of California, Irvine, with a spatial accuracy of 4 km was utilized in this study. Rainfall data was imported into ArcGIS as raster data and employed to create a rainfall map as shown in the Fig. 5E.

Topographic wetness index

The Topographic Wetness Index (TWI) plays major role within the hydrological system, providing as a reflection of potential groundwater seepage affected by the area's topographical features. It has proven crucial in pinpointing the extent and location of saturated sources adding to surface runoff generation. Therefore, areas with the highest TWI values are labeled as holding the most substantial groundwater potential. Many researchers have utilized TWI as a key factor to delineate groundwater potential areas^{45,46,51}. As highlighted in a study by Beven and Kirkby⁵², TWI connects ascending areas, acting as a measure of water flow towards a specific point (i.e., the local slope), thereby indicating subsurface lateral transmissivity. The TWI is determined using the following equation.

$$TWI = \ln \left(\frac{As}{\tan \beta} \right)$$

In this context, “As” represents the specific catchment area, and “ $\tan \beta$ ” corresponds to the slope angle at the given location.

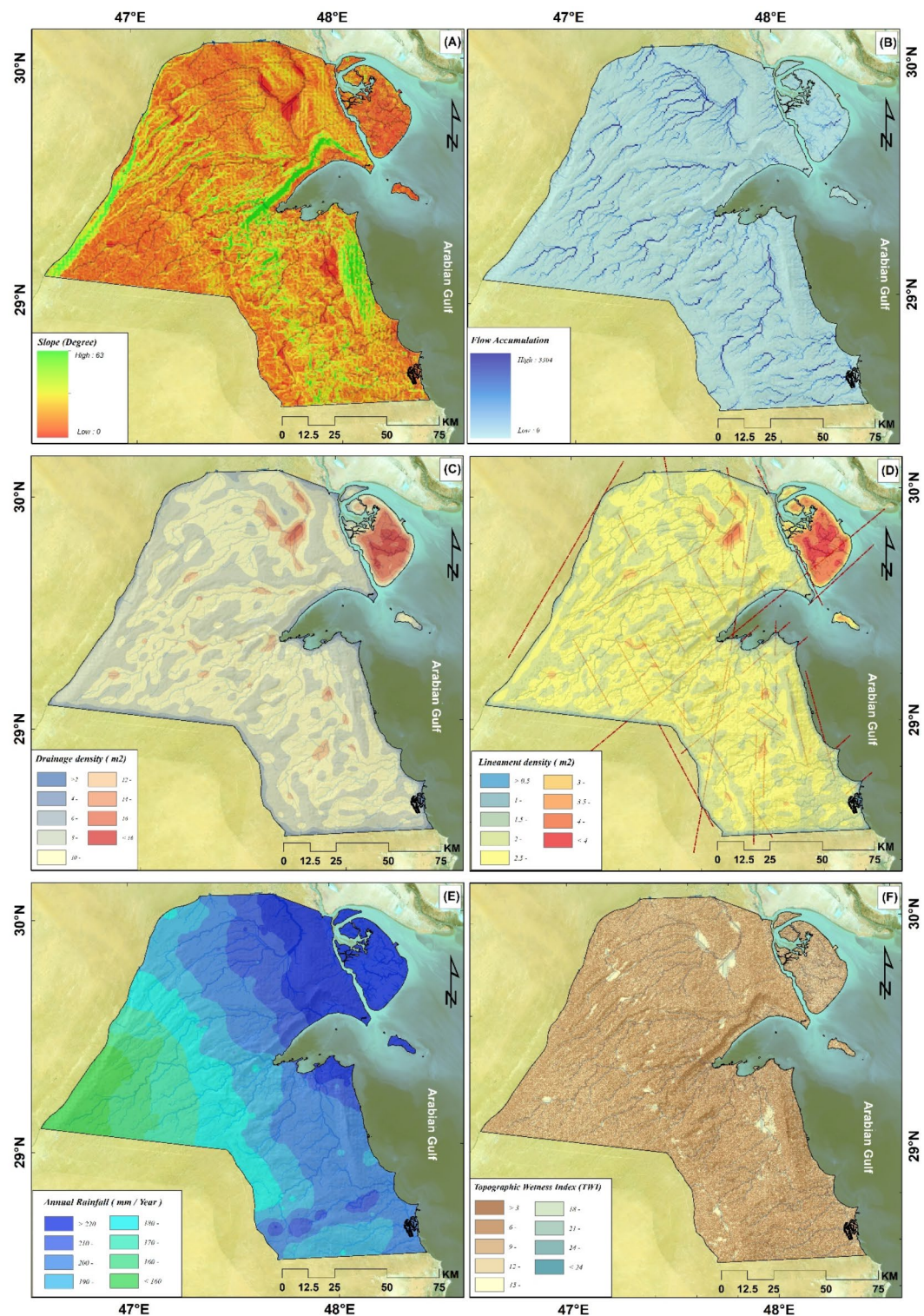


Fig. 5. Research area: (A) Slope; (B) Flow accumulation; (C) Drainage density; (D) Lineament density; (E) Annual Rainfall⁶⁵; (F) Topographic wetness index.

Groundwater depth

Groundwater depth presents the upper boundary of the saturated zone; therefore, the depth of the water table is a key element of the hydrological cycle in the region, alongside topography and rainfall patterns. Changes in groundwater pressure result in fluctuations in the water table level.

Land use and land cover

Land use and land cover (LULC) are essential factors affecting the groundwater recharge rate, surface runoff, and evaporation^{12,36}. This usage provides essential information on various topics such as leakage and recharge, soil moisture, and the distribution of surface and groundwater and their occurrence (da Costa et al., 2019). The LULC map data was obtained from the Global Land Cover database³⁷ with a 10-meter resolution as shown in the Fig. 6A. Subsequently, adjustments were made by cross-referencing field data and aerial photographs through ArcGIS 10.8 to ensure accuracy.

Geomorphology

The region's geomorphology is a fundamental element for dividing groundwater recharge areas, as it provides evidence of various shapes and processes, such as temperature fluctuations, groundwater movement, and geochemical interactions within the Earth's subsurface, and more^{24,56–58}. Seepage capabilities will affect the potential for groundwater recharge in different geomorphological units⁵⁹. Barchan Sand Dunes, Active Sand Sheets, Desert Floor Deposits, Siliciclastic Granule Lag, Fall Dunes, Deflated Rugges Sand Sheets, Smooth Sand Sheets, Gravel Lag, Barchanoid Ridges, Playa Deposits, Urban areas, Coastal Plain Deposits, Desert Floor Deposits Calcareous Debris are among the vital geomorphological features in the study area as shown in Fig. 3D.

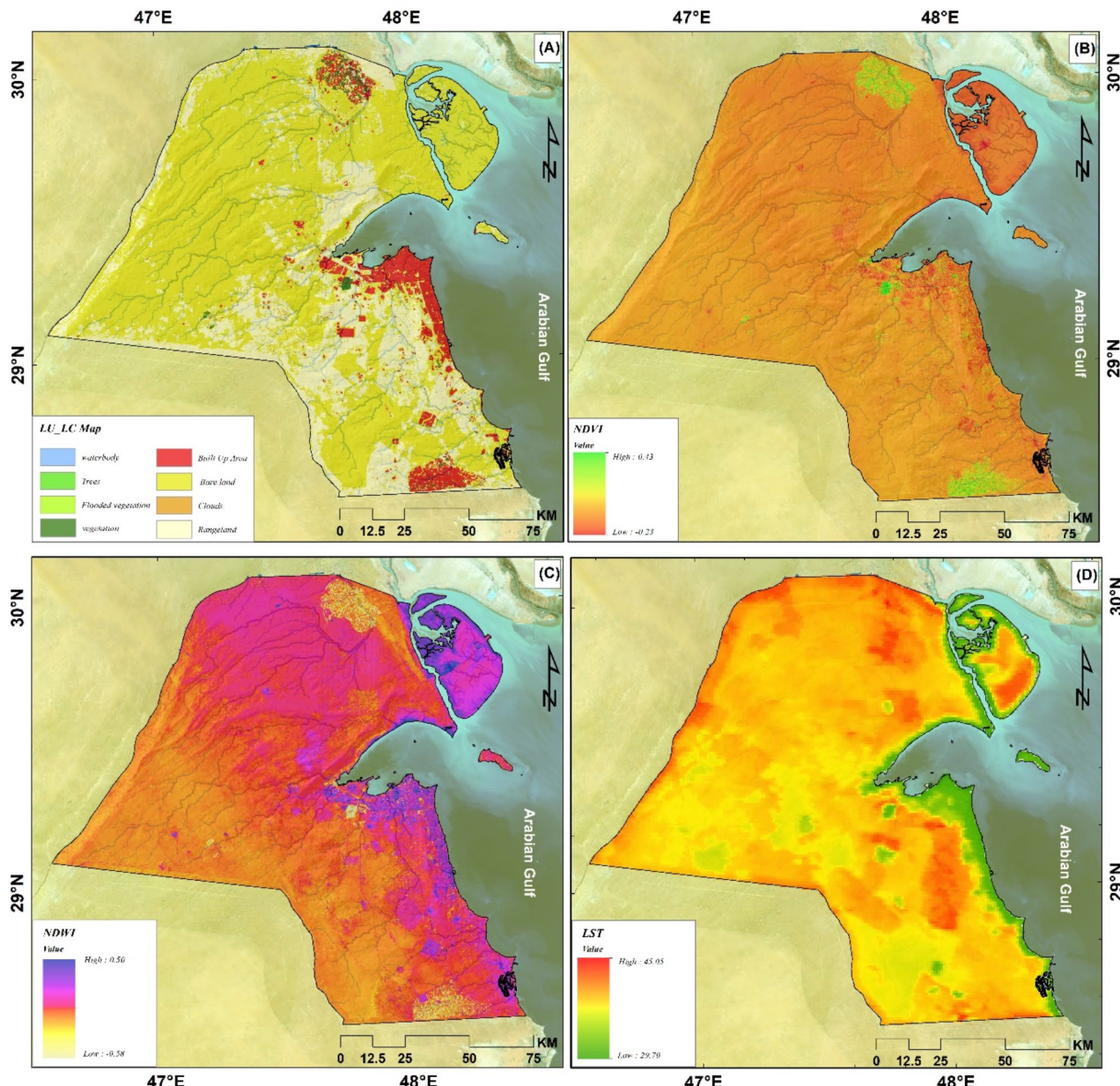


Fig. 6. Research area: (A) Land use and land cover; (B) Normalized differential vegetation index; (C) Normalized differential water index; (D) Land surface temperature.

Geology

The potential existence of groundwater major relies to geology features of the area. Geological features heavily influence groundwater's presence and distribution across an area. Rainwater struggles to seep through without suitable rock formations, and groundwater finds storing underground tricky. Water movement and storage capacity within groundwater layers vary based on rock characteristics like porosity and permeability^{6,44}. Different geological indicators results in a significant role in the movement and accumulation of groundwater, necessitating careful consideration in groundwater research. For instance, rocks like sandstone, which possess high porosity, efficiently retain water, whereas low-porosity rocks such as clay and oil-bearing formations have limited water storage capacity. Moreover, fractures and voids within rocks serve as vital conduits for guiding groundwater movement and facilitating its flow between rock layers⁶⁰.

Normalized differential vegetation index (NDVI)

NDVI is a reliable gauge of groundwater levels, particularly in these specific regions and ecosystems. Robust, lush vegetation with a high greenness index boosts groundwater recharge. This is achieved through the plant's canopy and root systems, intercepting rainfall, and slowing surface water runoff. Consequently, more water can seep into the soil, replenishing groundwater. Thus, a high greenness index can significantly increase groundwater recharge in vegetated areas. To assess Groundwater Potential (GWP) and identify land cover in the study area, a pixel-based NDVI within the range of -1.0 to +1.0 was computed in this research as shown in the Fig. 6B, utilizing the equation from Taloor et al.^{6,16,61,62} applied to Sentinel 2 based Google Earth Engine data.

$$\text{NDVI} = (\text{NIR} - \text{RED}) / (\text{NIR} + \text{RED}), \text{ where RED is B4, 664.5 nm, NIR is B8, 835.1 nm.}$$

Normalized differential water index (NDWI)

The NDWI is considered an effective tool for exploring potential groundwater areas, as the presence of water in the soil or vegetation serves as an indirect indicator of groundwater availability. When plants contain a high percentage of water, it increases the vegetation cover density, allowing more water to penetrate the soil, thus replenishing groundwater. Higher NDWI values are associated with increased groundwater nourishment, and areas with consistently high NDWI values are considered reliable groundwater sources. The role of the NDWI is more prominent in areas with high soil moisture content, indicating the presence of water in the soil. This indirectly serves as evidence of groundwater potential in the region. The NDWI in this study was calculated using the equation proposed by Liu et al.⁶³ and applied to data from the Google Earth engine based on Landsat 8. The formula used is $(\text{NIR} - \text{SWIR}) / (\text{NIR} + \text{SWIR})$, where NIR represents the near-infrared range and SWIR represents the shortwave infrared range. Generally, higher NDWI values indicate higher water content in the observed area as shown in the Fig. 6C.

Land surface temperature

Land surface temperature (LST) is a valuable indicator for assessing groundwater potential in a specific area, considering various environmental factors. Lower temperatures, often linked to vegetation and specific ground covers, may suggest conducive conditions for groundwater recharge. In urban settings, impervious surfaces like asphalt and concrete contribute to elevated ground surface temperatures, reducing groundwater recharge potential. Conversely, vegetation aids in cooling the land surface through shade and evaporation, enhancing groundwater possibilities in densely vegetated regions. In our study, Landsat 8 data was utilized to derive LST values, which were applied to Google Earth Engine data based on thermal bands from satellite images (bands 10 and 11). The process involved converting Digital Numbers (DN) to radiance using sensor calibration parameters, subsequently calculating brightness temperature per Planck's law (Eq. 1), followed by conversion to Land surface temperature using the Stefan-Boltzmann law (Eq. 2).

$$T_b = \frac{k_2}{\ln\left(\frac{K_1}{L} + 1\right)}$$

where: T_b is the brightness temperature, k_2 and K_1 are sensor-specific calibration constants, L is the radiance.

$$LST = \left(\frac{T_b}{\epsilon}\right)^{\frac{1}{4}}$$

Where: LST is the Land Surface Temperature, ϵ is the emissivity.

Methodology

Mapping the groundwater potential zone with conventional techniques is quite difficult. The lack of thematic layers in the traditional approach—such as data on soil, groundwater level, and geomorphology—causes problems. The absence of historical maps or data from pertinent departments and organizations makes the process of gathering data even more difficult. This makes it more difficult to validate the groundwater potential zone mapping's correctness and dependability. These difficulties bring to light the shortcomings and inadequacies of the conventional approaches used to carry out these mapping exercises. The creation of thematic layers using satellite data has become more commonplace recently for a variety of uses, such as mapping groundwater potential zones. Satellite imagery is a useful tool for obtaining information about vegetation indices, land cover, and other pertinent factors. Thematic layers obtained from satellite data can be used as a basis for groundwater potential analysis and assessment. This method enhances the final map's accuracy and dependability. Satellite

data were used to produce several thematic layers, such as: drainage density, slope, elevation, groundwater level, land use and land cover (LULC), geomorphology, soil, and drainage density.

Figure 7 illustrates the conceptual flowchart outlining the research design and methodology employed in this study. The flowchart delineates the automation process facilitated by Remote Sensing (RS) and Geographic Information System (GIS) software, accommodating spatial data variation between maps and remotely sensed data as shown in the Table 2 such as Alos PALSAR-DEM and satellite imagery. OpenStreetMap (OSM) serves as a valuable resource, offering user-acquired data freely accessible for download. Integration of OSM can enhance base maps while amalgamating diverse maps generated through remote sensing techniques. Furthermore, the proposed map delineates the preparation of data in a suitable format. According to the characteristics and multiplicity of spatial datasets used, the research methodology handle it while preprocessing the data using the data management resample tool in the Arc-GIS program; that tools allow controlling the cell size of the data that comes out of it, where all outputs were standardized to become in the cell size of 10 m, another preprocessing of data are conversion to raster tools (as polygon to raster or interpolation tools). The detailed steps of this methodology are elaborated in the subsequent sub-sections.

Working with topographic maps and satellite image analysis

The topographic map underwent geometric correction/georeferencing utilizing ESRI ArcGIS software, employing the Orthorectification process to mitigate spatial distortion and align the X and Y dimensions to a specific geographic reference system, the Universal Transverse Mercator (UTM) coordinate system—Datum: World Geodetic System (WGS 1984), Zone 39 North. Subsequently, the map was digitized onscreen, and its spatial data were saved in a vector formats as a feature classes geodatabase (Geo-Db). The Geo-Db was constructed using the ArcGIS program (Arc Catalog module) to generate various vector data types of the study area features: points, lines, and polygons. Identification and attribute data were then inputted. Following this, the spatial sub-setting process was applied to select and extract the entire raster data from the topographic map sheet using the spatial analyst toolbox/extraction toolset/extract by mask tool. Additionally, a more recent mapping of roads and other features within the studied area was conducted using ESRI Satellite Images.

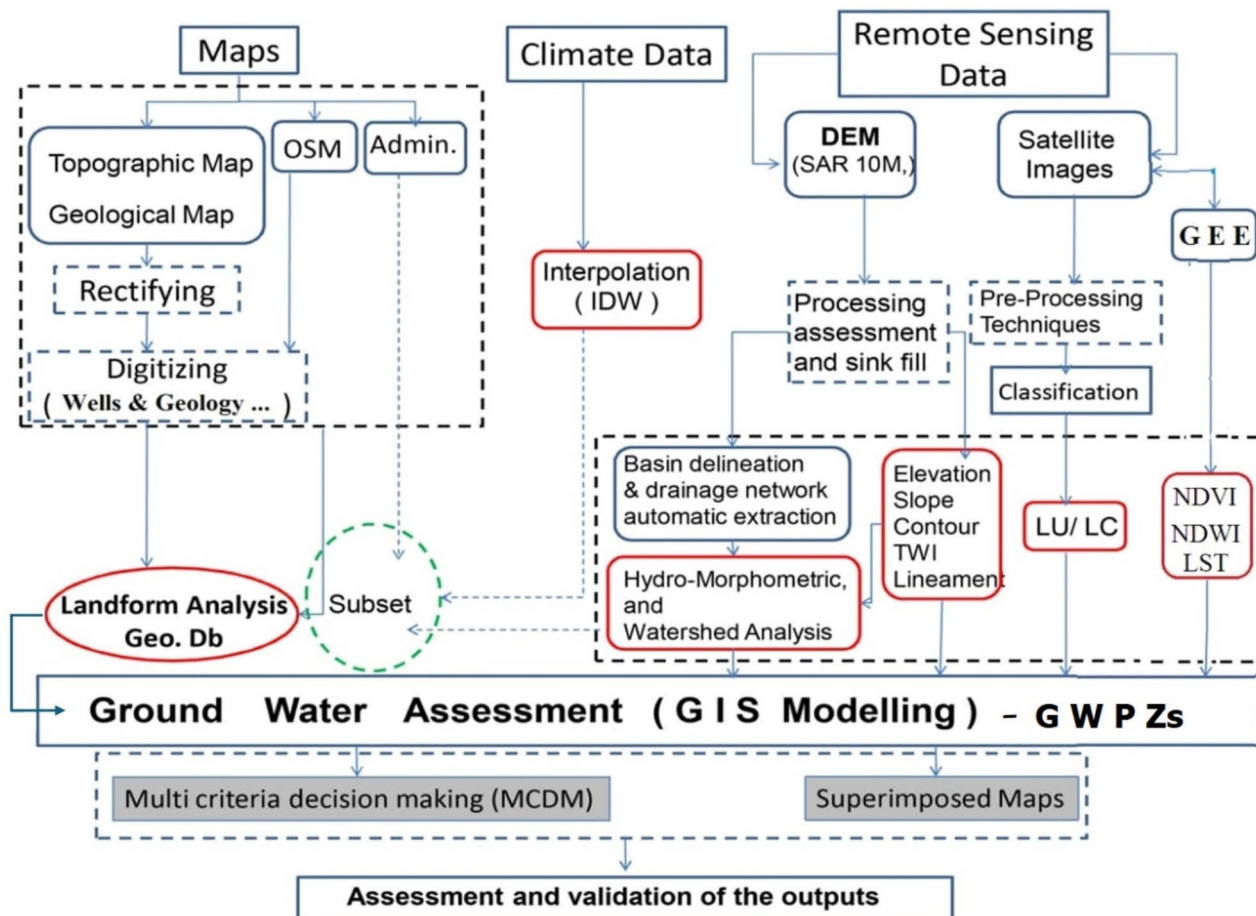


Fig. 7. Conceptual flowchart of this research is connected.

No.	Input data		Scale and spatial accuracy	Type of extracted data	Original Format Sources	Source
1	Geologic Data		1:10000	Geological map, Lineaments map	Vector	Kuwait Institute for Scientific Research (KISR), Kuwait – 1998 ³⁰
2	Geomorphology Data		1:10000	Geomorphology Units map	Vector	
3	Groundwater fields Groundwater wells		1:10000	Groundwater fields map	Vector	Kuwait Institute for Scientific Research (KISR), Kuwait – 2010 ³⁰
4	DEM (m)	ALOS PALSAR Terrain (Grid)	12.5 m	Slope, Aspect, Elevation, Hill shade, Curvature, Flow Direction, Flow Accumulation, Drainage Basins, Drainage Networks, and Topographic Wetness Index (TWI) maps	Raster	https://www.search.asf.alaska.edu ²⁹
5	Meteorological Data	Climate Data (2000–2022)	NA	Kuwait climatic conditions	CSV - text	https://www.power.larc.nasa.gov/data-access-viewer ⁶⁴
6		CHRS CCSCDR data	4 km	Yearly Rainfall Data (2000–2022)	Raster	https://www.chrsdata.eng.uci.edu ⁶⁵
7	Satellite Imageries	Land Sat 8-Oli (2018)	30 m 15 m	Normalize Difference Water Index (NDWI), Land Surface Temperature (LST) Utilizing GEE, AND Soil Moisture Index	Raster	USGS – Earth Explorer Website. https://www.earthexplorer.usgs.gov ⁶⁶
8		Sentinel 2b (2021)	20 m 10 m	Normalized Difference Vegetation Index (NDVI) Utilizing GEE and Sentinel-2 Land Use/Land Cover map produced by Esri (https://www.arcgis.com/home/item.html?id=d3da5dd386d140cf93fc9ecbf8da5e31)	Raster	https://www.sentinel.esa.int ⁶⁷
9	Groundwater data		1:10000	Ground-water level and total dissolved solids maps	Raster	³¹
10	Published Works	Papers, Reports	NA		Documents	NA

Table 2. The input data, spatial accuracy, and sources used in this study.

Working with digital elevation model

Studying terrain characteristics is crucial for the park's development process. A Digital Elevation Model (DEM) with a spatial resolution of 12.5 m was prepared for the study using data from the ALOS PALSAR Terrain. These data underwent preprocessing in ArcGIS software and were re-projected to align with the geographic coordinate system (UTM – Datum: WGS 1984 zone 39 N) for consistency with maps. The fill enhancement function was utilized to rectify errors in the digital elevation model (DEM). Additionally, a hydrology model was employed to generate the drainage network and basin watershed and boundary for the studied area.

Google earth engine

Scalable, cloud-based geospatial retrieval and processing are made possible by Google Earth Engine (GEE). Additionally, GEE offers free cloud-based computing capability for geospatial data analysis as well as access to the overwhelming majority of publicly accessible, multi-temporal Remotely Sensed data of satellite imagery and geospatial datasets (such as Landsat, Sentinel, and MODIS, ...etc.)⁶⁸. The geospatial community has embraced GEE recently and facilitated various local, regional, and global environmental applications. Maps depicting the world's changing forests are among the significant environmental applications for global urban change^{58,59}; GEE offers JavaScript and Python APIs for communicating with the Earth Engine servers to do computations. indices.

One sensor's worth of images is provided by Earth Engine and is compiled into a "collection" called image collection. Using a straightforward graphical user interface (GUI) and the Function.filter(), users can also define a point or polygon anywhere on Earth and filter image collection data from each satellite for user-defined time frames, area extent or location, and the percentage of an image pixel that is contaminated by cloud interference. They can also choose from a variety of predefined or custom image band combinations that align with the objective and research question. A script was created to filter date, check the cloud-free availability of images, preprocessing and calculation of used indices: NDVI, NDWI, and LST.

Weighting methods of criteria

This section offers an introduction to the Fuzzy Analytical Hierarchy Process (FAHP) and entropy-based aggregation methods employed to prioritize influential criteria from various experts' viewpoints.

This method can assist policymakers in setting priorities and producing appropriate outcomes. It is a helpful tool for resolving difficult decision-making challenges. By substituting a series of pairwise comparisons and findings for composite judgments, the AHP supports both subjective and objective aspects of a choice. Moreover, decision-making bias can be eliminated by using the AHP as a useful tool to evaluate the correctness of decisionmakers' assessments. It is predicated on the pairwise comparison between the selected criteria that is produced by the experts' assessment. To determine the relative importance of the most significant themes and their characteristics, views were solicited. There may be some disagreement because the comparisons are based on subjective or individual viewpoint. One of the most important benefits of the AHP is that it can be used to quantify the degree of consistency among paired comparisons of various criteria. This consistency ratio was found to be one way to verify that the perceptions are consistent. The AHP covers and integrates spatial data as input and produces decisions as output. By creating a pairwise comparison matrix with Saaty's scale, the qualitative data of many themes and attributes are converted into quantitative data^{69–72}. Weights were adopted that were consistent with the natural and environmental conditions of the study area, and criteria that were not included in similar areas and were applied in other areas of a different nature were modified to match the conditions of the study area according to consultation with experts and specialists.

Trapezoidal interval type II fuzzy Analytical Hierarchy process

Gupta and Lee⁵⁹ provided the trapezoidal Interval Type-2 Fuzzy Analytical Hierarchy Process (IT2 FAHP) approach. This method is used to provide the weights of the criteria in the analysis. Experts' responses, based on AHP are documented in decision matrices. These decision matrices are transformed into trapezoidal fuzzy numbers⁷³. Following this, the aggregated comparison matrix is constructed by calculating the arithmetic mean of the respondents' responses according to Eq. (1):

$$downrightZ_q = \left(\tilde{\tilde{x}}_{ij}^q \right)_{m \times n} = \begin{bmatrix} \tilde{\tilde{x}}_{11}^q & \cdots & \tilde{\tilde{x}}_{1n}^q \\ ?^q & \ddots & ?^q \\ \tilde{\tilde{x}}_{m1}^q & \cdots & \tilde{\tilde{x}}_{mn}^q \end{bmatrix}, 1 \leq i \leq m, 1 \leq j \leq n, 1 \leq q \leq k \quad (1)$$

Where; $\tilde{\tilde{x}}_{ij}^q$ represents the aggregated matrix of the upper and lower IT2 fuzzy sets, which should be calculated:

$\tilde{\tilde{x}}_{ij}^q = \left(\frac{\tilde{\tilde{x}}_{ij}^1 + \tilde{\tilde{x}}_{ij}^2 + \cdots + \tilde{\tilde{x}}_{ij}^k}{k} \right)$. Besides, k refers to the number of respondents. Equations (2–3) can be selected to obtain the upper (P^U) and lower (P^L) fuzzy matrices:

$$P^U = \begin{bmatrix} p(\tilde{A}_1^U \geq \tilde{A}_1^U) & \cdots & p(\tilde{A}_1^U \geq \tilde{A}_n^U) \\ ? & \ddots & ? \\ p(\tilde{A}_n^U \geq \tilde{A}_1^U) & \cdots & p(\tilde{A}_n^U \geq \tilde{A}_n^U) \end{bmatrix}, 1 \leq i \leq n \quad (2)$$

$$P^L = \begin{bmatrix} p(\tilde{A}_1^L \geq \tilde{A}_1^L) & \cdots & p(\tilde{A}_1^L \geq \tilde{A}_n^L) \\ ? & \ddots & ? \\ p(\tilde{A}_n^L \geq \tilde{A}_1^L) & \cdots & p(\tilde{A}_n^L \geq \tilde{A}_n^L) \end{bmatrix}, 1 \leq i \leq n \quad (3)$$

The ranking value of the upper membership function $Rank \left(\tilde{A}_i^U \right)$, lower membership function $Rank \left(\tilde{A}_i^L \right)$, and fuzzy set $Rank \left(\tilde{A}_i \right)$ are computed using Eqs. (4–6):

$$Rank \left(\tilde{A}_i^U \right) = \frac{1}{n(n-1)} \left(\sum_{k=1}^n p \left(\tilde{A}_i^U \geq \tilde{A}_k^U \right) + \frac{n}{2} - 1 \right), 1 \leq i \leq n \quad (4)$$

$$Rank \left(\tilde{A}_i^L \right) = \frac{1}{n(n-1)} \left(\sum_{k=1}^n p \left(\tilde{A}_i^L \geq \tilde{A}_k^L \right) + \frac{n}{2} - 1 \right), 1 \leq i \leq n \quad (5)$$

$$Rank \left(\tilde{A}_i \right) = \frac{Rank \left(\tilde{A}_i^U \right) + Rank \left(\tilde{A}_i^L \right)}{2}, 1 \leq i \leq n \quad (6)$$

Where; $\sum_{i=1}^n Rank \left(\tilde{A}_i \right) = 1$

Finally, Eqs. (7, 8) are used to normalize ranking values of the upper membership function (d_{ij}^U), lower membership function (d_{ij}^L). To calculate the relative weights, the fuzzy set's average normalized ranking value (d_{ij}) is computed using Eq. (9):

$$d_{ij}^U = \frac{Rank \left(\tilde{A}_i^U \right)}{\sum_{j=1}^J Rank \left(\tilde{A}_i^U \right)}, 1 \leq i \leq n, 1 \leq j \leq J \quad (7)$$

$$d_{ij}^L = \frac{Rank \left(\tilde{A}_i^L \right)}{\sum_{j=1}^J Rank \left(\tilde{A}_i^L \right)}, 1 \leq i \leq n, 1 \leq j \leq J \quad (8)$$

$$d_{ij} = \frac{d_{ij}^U + d_{ij}^L}{2} \quad (9)$$

Where; d_{ij} indicates the preference rating of the criteria and it shall be noted that $\sum d_{ij} = 1$.

MCDA suitability model according to entropy-based aggregation approach

Gupta and Lee⁵⁹ provided the trapezoidal Interval Type-2 Fuzzy Analytical Hierarchy Process (IT2 FAHP) approach. We used this approach to calculate the weights of the criteria in the analysis. The weighted average of each criterion (w_i^{avg}) can be defined using Eq. (10):

$$w_i^{avg} = \frac{\sum_{j=1}^m w_i^j \times S_j}{\sum_{j=1}^m S_j} \quad (10)$$

Where; S_j refers to the number of respondents in the j th group.

Measure the entropy value (E_j) for each group of respondents using Eq. (11):

$$E_j = \sum_{i=1}^n \left(\frac{-1}{\ln(2)} (w_i^j \times \ln(w_i^j) + w_i^{avg} \times \ln(w_i^{avg})) \right) \quad (11)$$

Where n refers to the number of criteria.

The diversification value (div_j) for each respondent and normalize these values (\bar{w}_j) to determine the significance level of each group using Eqs. (12, 13):

$$div_j = n - E_j \quad (12)$$

$$\bar{w}_j = \frac{div_j}{\sum_{j=1}^m div_j} \quad (13)$$

Calculate the compromise weight (cw_i) of criteria and rank the estimated weights in descending order to determine the most influential criteria using Eq. (14):

$$cw_i = \sum_{j=1}^m \bar{w}_j \times w_i^j \quad (14)$$

Finally, Table A (1) presents assigned weights and ratings based on each factor, while Table A(2) presents mutual independence and ratings among criteria with a consistency check of 10%.

Results

A comprehensive set of thirteen thematic maps was constructed to evaluate the groundwater potential in Kuwait. These maps encompassed data related to various factors such as geology, slope, rainfall, elevation, Normalized Difference Vegetation Index (NDVI), Normalized Difference Water Index (NDWI), Land Surface Temperature (LST), drainage density, Land Use and Land Cover (LULC), lineament density, topographic wetness index (TWI), geomorphology, and the water table. Creating these datasets involved combining remote sensing techniques and traditional data sources, utilizing software tools like ERDAS and ArcGIS.

Among these thematic maps, topographic elevation, slope, drainage density, and TWI maps were derived from ALOS PALSAR RTC data. The remaining maps were developed using data from various sources, including Landsat-8, SENTINEL-2 satellites, and conventional resources like geology, rainfall, water table, NDVI, NDWI, LST, and LULC maps. All converted layers underwent reclassification to ensure data consistency, aligning them with the study site's specific requirements. They were then resampled to establish a uniform cell size of 10 m. Reclassification simplified the interpretation of raster data by merging ranges of cell values into a unified value based on a consistent ranking system, with object (using value) in the ramp reclassify tool (spatial analysis tool-box in Arc-GIS software) is used to specify how to reclassify values of the input raster. This streamlined the process of comparing and ranking sites based on their suitability. Additionally, this study analyzed the relationship between the variables employed for predicting groundwater potential during the weight calculation and the actual groundwater potential.

Our DEM elevation analysis revealed that the highest point reached 290.94 m above sea level (ASL), and the lowest point descended 22 m below sea level. According to a study by Melese et al.⁵² and Hasanuzzaman et al.²⁵, coastal regions generally exhibit lower elevations, significantly impacting groundwater availability. Additionally, it is observed that lower elevations have a more significant influence on groundwater presence compared to higher elevations, leading to variations in climatic conditions. These variations can affect rainfall patterns, soil quality, vegetation types, land use, and coverage. To delve deeper into this analysis, as depicted in SM 1 (A), the terrain is categorized into nine classes based on elevation, assigning the lowest rank to nearly flat areas and the highest rank to those with relatively high runoff elevations. In summary, elevation emerges as a critical determinant of groundwater potential, holding a secondary position with a normalized weight of 0.066 about its impact on groundwater potential areas, as illustrated in Table A (1) based on the chosen factors in this study.

Slope results (Fig. 5A)) revealed that the study area predominantly exhibited slopes between 0° and 63°. Consequently, the surface slope was categorized into five classes on the slope map. The class with the lowest value was assigned a higher ranking due to its nearly flat terrain, while the class with the highest value was assigned

a lower ranking owing to its relatively high runoff levels. The slope is significant, with a normalized weight of 0.046, based on its relative influence on identifying potential groundwater areas among the selected parameters in this study as presented in Table A (1). Utilizing standard and customized weight values, the study area's slope was categorized into nine groups, with slopes less than 5 degrees indicating good potential. In contrast, those exceeding 40 degrees signify significantly low probability, as SM1 (B) illustrates.

Besides the slope, a comprehensive drainage analysis highlighted the runoff tributaries and the drainage density. Our results highlighted that drainage density values range from 0 to $17.6 \text{ m}^2/\text{km}^2$, as depicted in Fig. 5C. Among the selected parameters in this study, drainage density holds the third position with a normalized weight of 0.136 due to its relative importance in determining potential groundwater areas. Consequently, areas with low drainage density received higher scores, while regions with dense drainage received lower scores, as shown in Table A (1). The study area underwent reclassification into nine distinct categories for analytical purposes, unveiling a notable groundwater recharge potential despite its low drainage density. Regions characterized by low density exhibit a moderate capacity for recharge, whereas those with medium density demonstrate a lower recharging capability. Conversely, areas marked by high drainage density exhibit a notably low potential for groundwater recharge, as depicted in SM1 (C), Table A (1).

A structural analysis was performed through lineaments analysis, shown in Fig. 5D. The latter revealed that lineament density varied from 0 to $4.27 \text{ m}/\text{km}^2$. Lineament density emerged as the fourth most significant parameter in delineating groundwater potential zones in this study as indicated in Table A (1), with a normalized weight value of 0.037. The line density map revealed that the central part of the study area is highly suitable for groundwater due to the density of lineaments. In contrast, the western and the eastern regions have a lower potential for groundwater recharge as the lineament density decreases from the center towards the east and west as depicted in Fig. 5D. The study area underwent reclassification into nine clearly defined categories, revealing that regions characterized by low line density display diminished recharge capacity. Conversely, areas featuring high line density demonstrate a notable potential for groundwater recharge, as illustrated in SM 1(D) and Table A (1).

The rainfall results are one of the most critical factors in the current research. Our findings revealed that the average annual precipitation varies between 39.8 mm and 107.1 mm. A map with satisfactory outcomes was created using the inverse distance weighting (IDW) method. Consequently, regions in the north, receiving the most rainfall, were rated the highest, while ratings diminished towards the southern areas. Figure 5E illustrates the rainfall map categorization, adjusted to a 10 m^2 spatial resolution, and segmented into nine subclasses through a natural fraction classification technique. Regions with scant precipitation were depicted as having minimal recharge potential, whereas those experiencing abundant rainfall were deemed to possess high recharge potential, as shown in SM 1(E). Given the substantial influence of rainfall on potential areas, it was attributed to a high weight of 0.042, as determined among the selected parameters in this study (Table A1).

Besides the rainfall results, TWI was calculated to enhance our results. Figure 5F visually depicts the range of Topographic Wetness Index (TWI) values in our investigation, which spanned from -13 to 27 within the study area. These values were subsequently categorized into nine groups for further analysis. Higher weights were assigned to high topographic wetness index values and, conversely, lower significance to lower values, as illustrated in SM1 (F). Given the significant impact of the topographic wetness index on potential groundwater areas, a substantial weight of 0.206 was allocated to it, as determined among the selected parameters in this study Table A (1).

Rainfall is also a significant contributor to fluctuations in the groundwater level, as it serves as a source of recharge to the groundwater layer, replenishing it from rainfall. Thus, a depth-to-water table analysis was performed based on previous studies. It is well-known that changes in the water table within the region's topography primarily result from variations in rainfall patterns, groundwater recharge, and discharge^{34,35}. Groundwater in Kuwait is predominantly characterized by two distinct aquifers: the Kuwait Group aquifer and the Dammam aquifer. As illustrated in Fig. 3E, the water table depth in Kuwait ranges from 2 to 30 m, with the map displaying a gradual decline in the water table depth towards the outlet in the study area. Higher weights were assigned to lower water table depths and vice versa. Values were reclassified into nine categories, as shown in SM2(A). Given the significant impact of the water table depth on potential groundwater areas, a substantial weight of 0.125 was assigned to it, as determined among the selected parameters in this study Table A(1).

LULC analysis is considered one of the most common investigations in groundwater potentiality mapping in recent years. Our results revealed that The LULC map for the studied area consists of seven main categories, which are Water, Trees, Flooded vegetation, Crops, Built Area, Bare ground, and Rangeland, as shown in Fig. 6A land use patterns in the study area. Water bodies and agricultural land are excellent sources for groundwater recharge because they favor rainwater filtration and an increased rate of groundwater replenishment. In contrast, arid and built-up areas are considered less important in this context. The data indicates their contribution to increased surface runoff, reduced leakage rates, and decreased groundwater replenishment. For this reason, classifications have been assigned according to the available water quantity for replenishment based on land surface characteristics. Agricultural lands were given the highest rating of 0.00%, paved built-up areas were given the lowest rating of 0.25%, and water bodies were assigned a classification coefficient of 0.11%. Higher weights were allocated to these categories in the following order: Vegetation, Trees, Flooded vegetation, waterbody, Rangeland, Bare land, Built Up Area, and Clouds, respectively, as shown in SM2 (B) in terms of their impact on groundwater replenishment Table A (1). LULC is ranked with a natural weight of 0.021 based on its relative impact on potential groundwater areas, as determined among the selected parameters in this study Table A (1).

Besides the previous factors, geomorphological and geological features were analyzed to highlight recharge capabilities within the study area, as shown in SM2(C). The latter denotes grades assigned based on the recharge capabilities of different geomorphological areas. Subsequently, subjective weights were assigned based on the characteristics of each layer. Coastal Plain Deposits and Sand and Gravel deposits were rated highly due to their

excellent permeability, receiving a grade of nine. Conversely, Playa Deposits and Urban areas, known for their high water-holding capacity, were given a lower grade of one. Highlands and plateaus influenced this decision and typically facilitate surface runoff. Geomorphology is positioned with a natural weighting of 0.052, reflecting its relative impact on potential groundwater zones within the specified parameters of this study Table A (1). Geologically, our results and findings depend mainly on the rock units' distribution in Fig. 3C. Utilizing the Analytic Hierarchy Process (AHP) framework, the resultant geological map underwent reclassification into nine primary categories based on their hydrogeological characteristics, as depicted in SM 2 (D). Geology is positioned with a natural weighting of 0.026, reflecting its relative impact on potential groundwater zones within the specified parameters of this study Table A(1).

One of the most critical factors affecting GWPZ is NDVI. Our results of NDVI through GEE highlighted that the resulting NDVI map values (see Fig. 6B) span from –0.22 to 0.43, with values exceeding 0.4, signifying the presence of dense vegetation. Values lower than 0.15 indicate an absence of vegetation, such as barren land and sand, while values below zero indicate urban areas and water bodies, as noted by Rulinda et al.³⁹. The NDVI images were subsequently classified into nine groups, revealing differences in the distribution of plants between parts of the study area, and they are spread in the Abdali area in northern Kuwait, Al-Wafra in southern Kuwait, and the Sulaibiya agricultural area as shown in SM3 (A). NDVI is positioned with a natural weighting of 0.121, reflecting its relative impact on potential groundwater zones within the specified parameters of this study Table A(1).

Additionally, and using GEE, NDWI was calculated to strengthen our results. The resulting NDWI map values range from –0.58 to 0.50, as shown in Fig. 6C. Subsequently, the NDWI images were classified into nine groups, revealing differences in surface water distribution among different parts of the study area. These differences are apparent in the eastern part of the country (See SM3 (B)). NDWI is positioned with a natural weighting of 0.046, reflecting its relative impact on potential groundwater zones within the specified parameters of this study Table A(1).

Besides all the previous factors, LST was studied as an indicator for GWPZ, where the lower the LST, the higher the probability of closer groundwater zones to the surface. The resulting LST map values range from –0.58 to 0.50, as shown in Fig. 6D. Subsequently, the LST images were classified into six groups, revealing differences in surface water distribution among different parts of the study area. These differences are apparent in the eastern part of the country (See SM3 (C)). LST is positioned with a natural weighting of 0.076, reflecting its relative impact on potential groundwater zones within the specified parameters of this study Table A(1).

Groundwater potential zones (GWPZs)

The results of the previous factors were spatially analyzed to check the GWPZs within the study area. Our spatial overlay analysis and weighted analysis findings are introduced in Fig. 8; Table 3. Based on these two supported results, groundwater potential zones in the north and east parts of Kuwait are very highly suitable. However, very high suitability is less than 1.5%, and suitable zones with high and moderate degrees cover 12% and 37%, respectively. Based on input data, these are logical results since rainfall, NDVI, NDWI, and LST impact results in this area. Lower parts of the country have higher chances of groundwater potential. Shallow The low potential covers nearly 50% of the country's area, covering more than 7500 km².

Verification for GWPZs

Field verification and statistical validation (kappa coefficient) were integrated to check the reliability of our methodology and confirm our research findings (Locations of GWPZs). The Kappa coefficient, commonly used to estimate interrater reliability, can be employed in the context of test–retest. In the test–retest, the Kappa coefficient indicates the extent of agreement between frequencies of two sets of data collected on two different occasions. Using this formula:

$$K = \frac{P_{agree} - P_{chance}}{1 - P_{chance}} \quad (15)$$

P agree shows the proportion of trials in which judges agree, and P chance shows the proportion of trials in which agreement would be expected due to chance⁷⁴. If the results are from 0.81 to 1.00, it shows almost perfect agreement, while 0.61 to 0.80 shows substantial validation quality. Based on the mentioned Table 4, the Kappa coefficient of the suitability scale is presented. Results indicate very high agreement results.

Field verification is presented in Fig. 9. According to results shown in Figs. 8 and 9, and Table 4 (kappa coefficient), it is clear how the utilized methodology delivered successful findings through the excellent matching between the locations of water wells and highly potential GWZs. Based on Table 4, a high suitability scale of 0.77 indicates 49 wells in that area. If we compare the results with Fig. 9A,B, most of the wells are found in very high groundwater potential zones (beige color), and significant parts are in high groundwater potential zones (yellow). Table 4, a very high suitability scale, shows the density ratio of 0.076 wells per km², suggesting that the highest value of existing wells is on the high suitability scale. This could mean that the kappa coefficient of 0.76 was not correctly calculated. However, the suitable area size for a suitable area size for a high suitability scale, suppose we check the appropriate area size for a high suitability scale. In that case, the results show that the area size suits a high suitability scale. We get logical results, and it can be concluded that our research is defined and conducted correctly.

The minimum highest areas (central west area) are the highest. The minimum distribution of wells is located in the highest areas (central west area), consistent with the research area's geology, geomorphology, and digital elevation model. Also, it indicated low shallow, shallow groundwater potential zones (Figs. 8 and 9). These results are in harmony with Tables 3 and 4. Based on the utilized approach and validation methods, our results

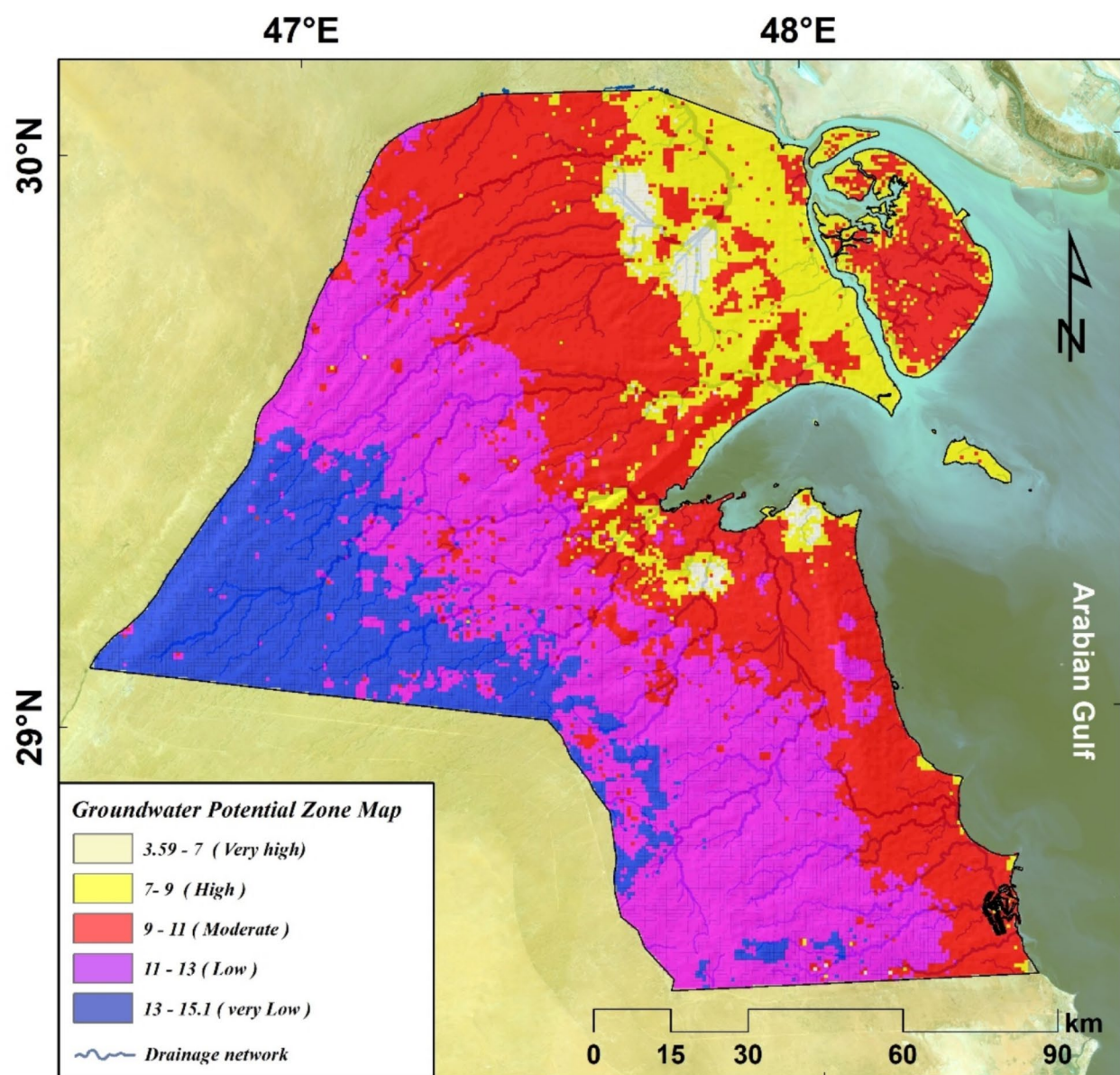
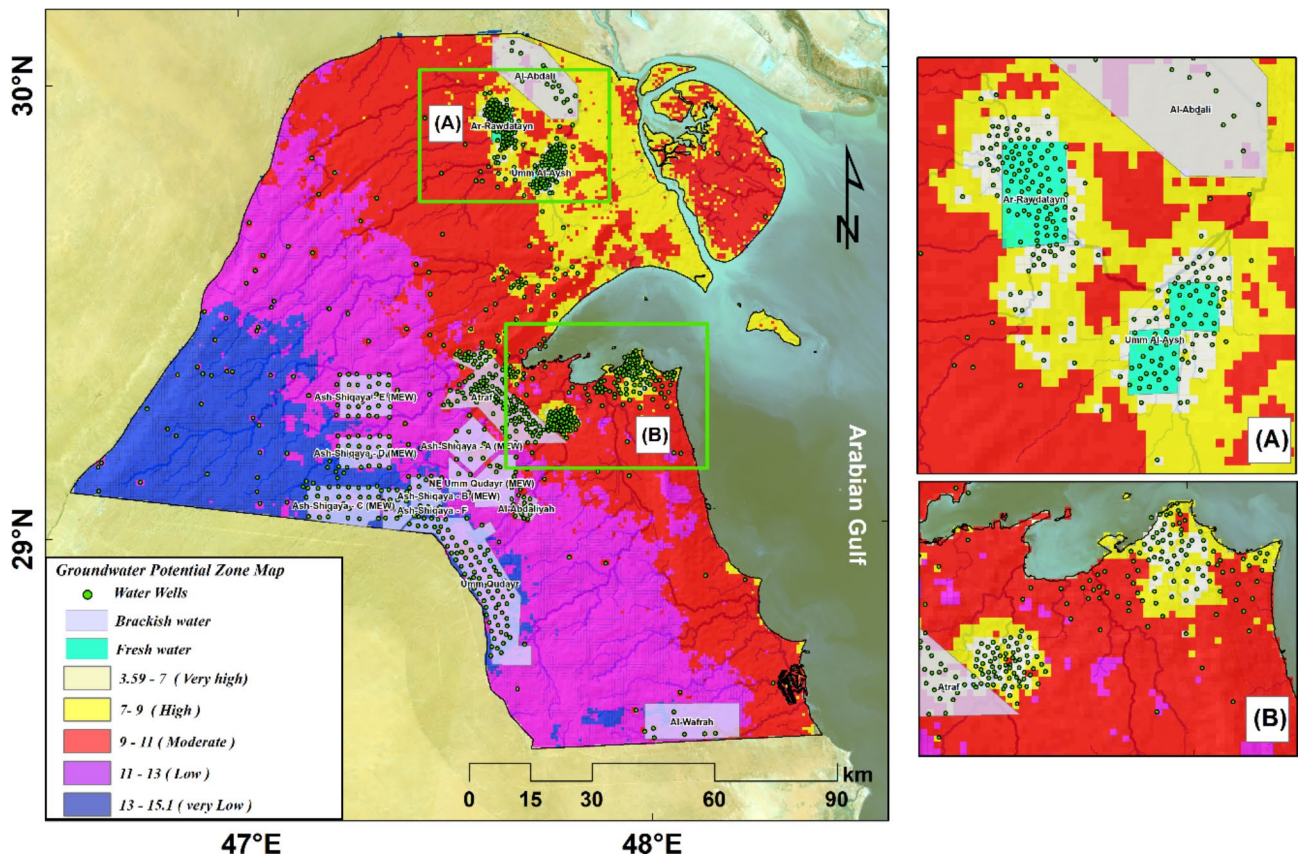


Fig. 8. Mapping of Groundwater potential zone levels in Kuwait.

No.	Class		Area km ²	%
	Value	Suitability degree		
1	3.59-7	Very high	241.176	1.393641
2	7-9	High	2151.328	12.4315
3	9-11	Moderate	6372.148	36.8216
4	11-13	Low	5933.602	34.28746
5	13-15.1	Very low	2607.204	15.06579
Total area			17305.46	100

Table 3. Suitability degree.

Suitability scale	Wells No.	Area (Km ²)	Wells Density (Well/Km ²)	Kappa coefficient
Very Low	119	2570.1	0.046	
Low	188	6013.01	0.031	
Moderate	367	6743.7	0.054	
High	49	1895.2	0.026	
Very High	201	264.7	0.076	0.76
Total	929	17486.71	0.053	0.77

Table 4. Kappa coefficient.**Fig. 9.** Field validation points (water wells) zones match the high potential zones.

show a considered show a considered show a considered shows how a considered show a considerable degree of consistency. Furthermore, our methodology could be applied not only in Kuwait but also in similar research areas in the world.

Discussion

This section will focus on addressing the comparison of our findings with literature that studied groundwater potential in Kuwait focusing mainly on their applied methodology and findings as shown in Table 5. The table highlights the utilized methods and findings for several hydrological and hydrogeological studies dealing with the characterization of water resources in Kuwait over the last 3 decades. This table highlights the novelty of our research on Kuwait, as we did not find any recent studies characterizing groundwater resources in Kuwait by integrating several datasets (geological, hydrological, climatic, etc.) using advanced multicriteria analysis and implementing web-based tools, e.g., GEE.

Extensive efforts were made to compile detailed information on groundwater yield and the primary agricultural fields reliant on groundwater resources. Our findings confirm significant groundwater usage in the regions identified as high-potential zones. Figure 10a-d highlighted the distribution of agricultural fields and their associated irrigation wells. These wells are predominantly situated within the high-potential groundwater zones identified in our analysis, providing a robust cross-validation of our results. This integration

Study	Methodology	Results
Al-Ruwaih and Khan (1993)	Hydrogeological and hydrochemical analysis	Identified salinity issues and evaluated the Dammam Aquifer's potential as a groundwater source.
Khalaf et al. (1986)	Geological and hydrogeological assessment	Investigated the water-bearing capacity of the Kuwait Group Aquifer, revealing factors affecting groundwater availability.
Nasr and Al-Ansari (2015)	Remote sensing and GIS application	Detected potential groundwater zones, demonstrating modern approaches for water resource identification in Kuwait.
Mukhopadhyay and Al-Haddad (2003)	Analysis of climatic data and recharge rates	Showed that limited rainfall and climatic variability significantly affect groundwater recharge sustainability.
El-Hames and Abdalla (2007)	Salinity assessment and usability evaluation	Evaluated groundwater salinity levels, proposing desalination and blending techniques for agricultural use.
Abdalla and Al-Rashed (1998)	Risk assessment of groundwater extraction	Discussed risks of over-extraction, emphasizing aquifer depletion and increased salinity concerns for sustainability.
Al-Ruwaih (1994)	In-depth hydrogeological investigation	Analyzed major aquifers' characteristics, detailing groundwater behavior in Kuwait.
Mukhopadhyay and Al-Sulaimi (1993)	Overview of hydrological conditions	Discussed general hydrology and hydrogeology, focusing on aquifer behavior and high salinity challenges.
Al-Mutairi and Abahussain (2014)	Groundwater quality evaluation	Comprehensive assessment revealing pollutants such as nitrates and heavy metals, with implications for water safety.
Al-Senafi and Anis (2015)	Evaluation of climate change impacts	Found that changing rainfall patterns affect groundwater recharge rates and resource sustainability.
Mukhopadhyay et al. (2000)	Discussion on artificial recharge strategies	Proposed techniques for artificial recharge of aquifers, emphasizing potential benefits for water resource management.
Saeed et al. (2008)	Impact assessment of urbanization	Examined how urbanization and industrial activities degrade groundwater quality in Kuwait.
Elango and Kalyanasundaram (2004)	Hydrochemical and isotopic analysis	Assessed groundwater origin and movement, providing insights into quality variations across regions.
Al-Ruwaih (1995)	Hydrogeological study of the Dammam Formation	Focused on the hydrological characteristics and quality of one of Kuwait's primary groundwater sources.
Mukhopadhyay et al. (1994)	Mathematical modeling of groundwater flow	Simulated groundwater flow conditions, offering insights into hydrological dynamics in Kuwait's aquifers.
Sen and Al-Sulaimi (1999)	Recharge rate estimation study	Investigated recharge rates in Kuwait's arid environment, providing crucial data for water management strategies.
Mukhopadhyay and Al-Awadi (2004)	Vulnerability assessment of aquifers	Discussed aquifer contamination risks, analyzing hydrological characteristics affecting groundwater vulnerability.
Al-Senafi and Anis (2017)	Interaction study of climate and hydrology	Analyzed how climatic and hydrological factors influence groundwater recharge rates in Kuwait.
Abderrahman (2000)	Comprehensive hydrology study	Focused on Kuwait's water resources management challenges in an arid climate, emphasizing groundwater issues.
Al-Rashed and Sherif (2001)	Hydrology review and future demand assessment	Reviewed groundwater hydrology and assessed future water demand in relation to available resources.
Current research	Thirteen criteria (rainfall, NDVI, geology, etc.) integrated GEE& AHP-MCDM	Kuwait's groundwater potential is strongest in the north and east, with high and moderate suitability zones covering 12% and 37%, respectively, while areas of extremely high suitability account for less than 1.5%

Table 5. Overview of Groundwater studies and findings in Kuwait.

further substantiates the accuracy and relevance of the identified groundwater potential zones for agricultural applications.

Our research offers valuable insights into managing groundwater resources in Kuwait's semi-arid regions, crucial for sustainable agriculture. By identifying high-potential groundwater zones using Google Earth Engine and MCDM, we provide a framework that can guide water resource allocation and agricultural planning. The findings suggest targeted groundwater extraction in areas such as the north and east, which would optimize water use for crops. Policy recommendations include promoting efficient irrigation practices, integrating groundwater with other water sources like treated wastewater, and enforcing groundwater monitoring to prevent overuse. These strategies align with Kuwait's Vision 2035 for enhancing food security and agricultural sustainability.

Future research should consider the impact of climate change on groundwater availability and explore additional datasets to refine predictions. Technological advancements, such as AI-driven models, could further improve groundwater management. Limitations include data accuracy and the regional specificity of the study, which may require adjustments for broader applications. Despite these, our study provides a practical, data-driven approach for optimizing water resources, with immediate implications for policymakers in Kuwait.

Conclusions and recommendations

In a Semi-Arid Region of KUWAIT, groundwater potential zone was detected using Multi-Criteria Decision Making. Analyzing several previous types of research and all sorts of studies evaluating groundwater potential zones, thirteen criteria were studies evaluating groundwater potential zones; thirteen criteria were selected to incorporate multicriteria decisions. The highest assigned weight is on rainfall, 0.162; topographical wetness index, 0.13; and NDVI, 0.122. Based on different input weights, different results emerge. However, the main idea is to find the perfect combination of parameters and weights. The main idea is to see an ideal combination of parameters and weights to evaluate groundwater potential. Comparing our results to other studies is

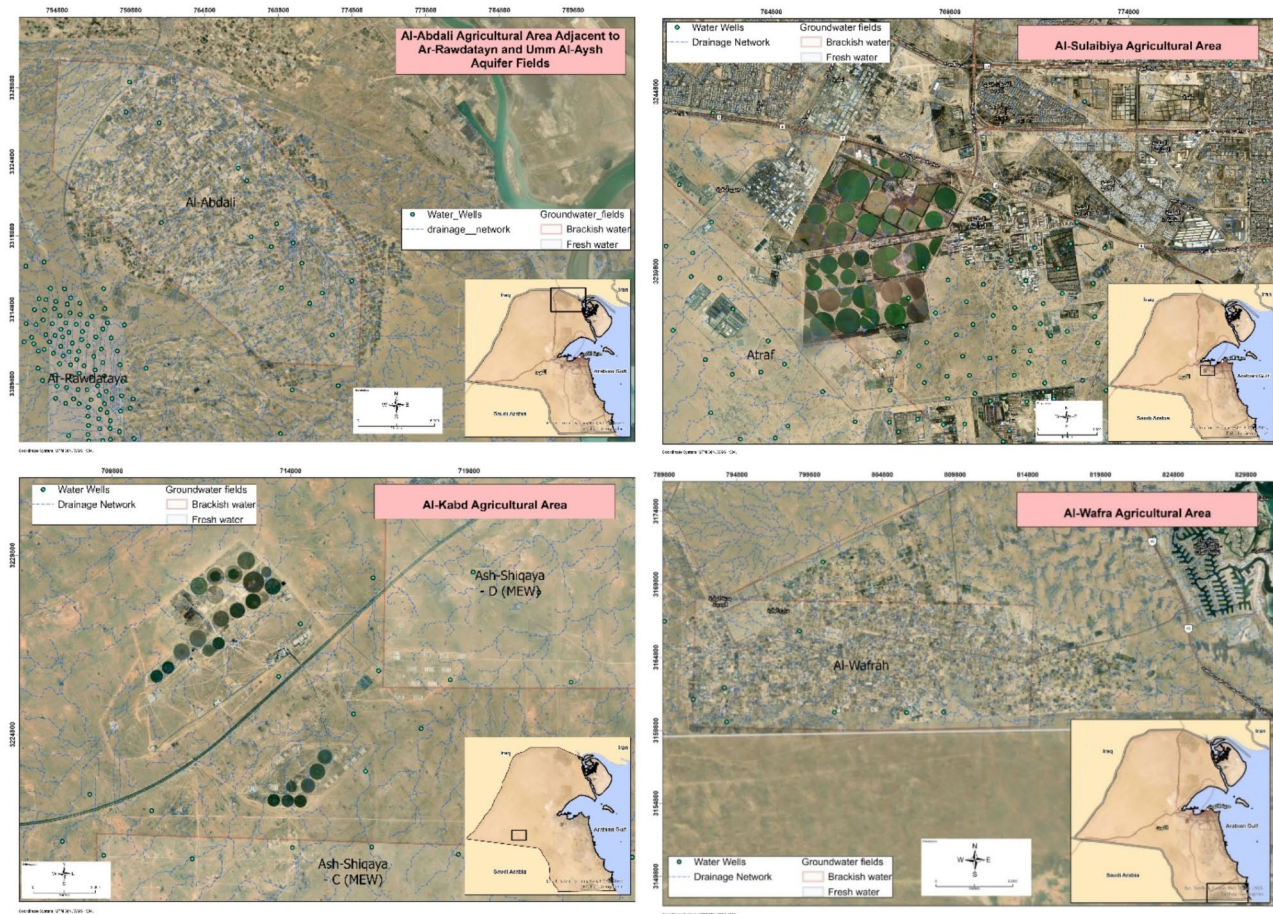


Fig. 10. Distribution of agricultural fields and associated irrigation wells.

almost impossible due to the different parameters used, the various parameters used, and the area's specific characteristics. However, some similarities can be drawn to other authors on similar (larger scale) areas.

The topographic wetness index with rainfall has the most effect on the research and detects the most impact on the research study of groundwater potential in semi-arid regions. Our research shows that combining more factors can increase precision while ensuring the stability of the detection process of groundwater potential zones. Another indication of quality research is. It shows the kappa values of suitability scale ranks and the kappa values of suitability scale ranks, which show substantial kappa coefficient values of 0.76 and 0.77, respectively. Our research concluded that a high degree of suitability for groundwater potential in Kuwait's semi-arid region is 242 km^2 .

Locations, areas, and water wells of very high and high potential zones are located in the northeast part of the research area and also in the south part of the research area in Kuwait. This is presented in our research and ground-validated and ground-validated. The latest research findings offer valuable insights for both public and commercial entities involved in groundwater management, land use planning, and environmental conservation within the researched area. Furthermore, the methodology employed in this study can be adapted to analyze similar watersheds sharing comparable hydrogeologic, topographic, and climatic attributes. Various strategies, such as enhancing groundwater replenishment, augmenting water supply, and implementing rainwater harvesting initiatives in urban settings, can improve water resource management. Additionally, using advanced geospatial techniques is imperative to manage water resources better, curb overexploitation, and explore untapped areas effectively. A more comprehensive multidisciplinary approach is advocated to refine groundwater potential zone mapping techniques, thereby fostering sustainable water resource management. Future research endeavors need to scrutinize the effects of climate change and urbanization on groundwater recharge and potential. Incorporating advanced remote sensing data like LIDAR, machine learning algorithms, real-time monitoring, and an integrated approach is recommended for future groundwater potential zone mapping, ensuring the system's sustainability. Emphasis is placed on conducting further research encompassing socioeconomic dimensions, long-term monitoring, field validation, and extending the scope to different geographical regions. Such future undertakings are pivotal in promoting sustainable water resource management, meeting the escalating water demands across various industries, and advancing global understanding of groundwater potential.

Data availability

The datasets used and/or analysed during the current study available from the corresponding author on reasonable request.

Received: 4 July 2024; Accepted: 18 October 2024

Published online: 02 December 2024

References

1. Todd, D. K. & Mays, L. W. *Groundwater Hydrology* (Wiley, 2004).
2. Tariq, M. A. U. R., Alotaibi, R., Weththasinghe, K. K. & Rajabi, Z. A detailed perspective of water resource management in a dry and water scarce country, *Case Kuwait* **10**, 1–20. <https://doi.org/10.3389/fenvs.2022.1073834> (2022).
3. Aliewi, A., Al-Kandari, J., Al-Khalid, A., Bhandary, H. & Al-Qallaf, H. Modelling the effect of high level of total dissolved solids (TDS) for the sustainable utilization of brackish groundwater from saline aquifers in Kuwait. *Environ. Dev. Sustain.* **23**, 2204–2223 (2021).
4. Arnous, M. O., El-Rayes, A. E., Geriesh, M. H., Ghodeif, K. O. & Al-Oshari, F. A. Groundwater potentiality mapping of tertiary volcanic aquifer in IBB basin, Yemen by using remote sensing and GIS tools. *J. Coast Conserv.* **24**, 1–20 (2020).
5. Ashmawy, M. H., El-Wahed, A., Mohamed, A., Kamh, S. Z. & Shebl, A. Comparative study of the drainage basin morphometry extracted from topographic maps and SRTM DEMs: An example from Ghadir watershed, Eastern Desert, Egypt. *Delta J. Sci.* **39**(2), 52–64 (2018).
6. Shebl, A. et al. Multi-criteria ground water potentiality mapping utilizing remote sensing and geophysical data: A case study within Sinai Peninsula, Egypt. *Egypt. J. Remote Sens. Sp Sci.* **25**(3), 765–778 (2022).
7. Mallick, J. et al. Modeling Groundwater potential zone in a Semi-arid Region of Aseer using Fuzzy-AHP and geoinformation techniques. *Water* **11**(12), 2656. <https://doi.org/10.3390/w11122656> (2019).
8. Mohammed, O. A. et al. Geoinformatics-based approach for aquifer recharge zone identification in the western Desert of Iraq. *GEOMATE J.* **25**(110), 220–234 (2023).
9. Sameer, Y. M., Abed, A. N. & Sayl, K. N. Geomatics-based approach for highway route selection. *Appl. Geomatics* **15**(1), 161–176. <https://doi.org/10.1007/s12518-023-00495-x> (2023).
10. Mohammed, S. S., Sayl, K. N. & Kamel, A. H. Ground water recharge mapping in Iraqi western desert. *Int. J. Des. Nat. Ecodyn.* **17**(6), 913–920 (2022).
11. Mohammed, O. A. & Sayl, K. N. Determination of Groundwater potential zone in arid and semi-arid regions: A review. In *13th International Conference on Developments in eSystems Engineering (DeSE)* 76–81 (2020).
12. Ozdemir, A. GIS-based groundwater spring potential mapping in the Sultan Mountains (Konya, Turkey) using frequency ratio, weights of evidence and logistic regression methods and their comparison. *J. Hydrol.* **411**, 3–4 (2011).
13. Naghibi, S. A., Pourghasemi, H. R., Pourtaghi, Z. S. & Rezaei, A. Groundwater Qanat potential mapping using frequency ratio and Shannon's entropy models in the Moghan watershed, Iran. *Earth Sci. Inf.* **8**, 171–186 (2015).
14. Das, S. & Pardeshi, S. D. Integration of different influencing factors in GIS to delineate groundwater potential areas using IF and FR techniques: a study of Pravara basin, Maharashtra, India. *Appl. Water Sci.* **8**, 1–16 (2018).
15. Kumar, M., Singh, P. & Singh, P. Integrating GIS and remote sensing for delineation of groundwater potential zones in Bundelkhand Region, India. *Egypt. J. Remote Sens. Sp Sci.* **25**(2), 387–404 (2022).
16. Ibrahim-Bathis, K. & Ahmed, S. A. Geospatial technology for delineating groundwater potential zones in Doddahalla watershed of Chitradurga district, India. *Egypt. J. Remote Sens. Sp Sci.* **19**(2), 223–234. <https://doi.org/10.1016/J.EJRS.2016.06.002> (2016).
17. Nigussie, W., Hailu, B. T. & Azagegn, T. Mapping of groundwater potential zones using sentinel satellites (–1 SAR and –2A MSI) images and analytical hierarchy process in Keta watershed, Main Ethiopian Rift. *J. African Earth Sci.* **160**, 103632. <https://doi.org/10.1016/J.JAFREARSCI.2019.103632> (2019).
18. Abdulkerim, E., Fufa, F. & Takala, W. Identification of groundwater recharge site using geographical information system and remote sensing: Case study of Sude district, Oromia, Ethiopia. *Environ. Earth Sci.* **81**(2), 1–15. <https://doi.org/10.1007/s12665-02-210170-w> (2022).
19. Agarwal, E., Agarwal, R., Garg, R. D. & Garg, P. K. Delineation of groundwater potential zone: An AHP/ANP approach. *J. Earth Syst. Sci.* **122**(3), 887–898. <https://doi.org/10.1007/s12040-013-0309-8> (2013).
20. Abebese, S., Anornu, G. K., Kabo-Bah, A. T., Dekongmen, B. W. & Sunkari, E. D. Assessment of groundwater potential zones using GIS and remote sensing techniques in the Bole District, Savannah Region, Ghana. *Int. J. Energy Water Resour.* **6**(4), 445–456. <https://doi.org/10.1007/s42108-022-00207-y> (2022).
21. Doke, A., Zolekar, R. B., Patel, H. & Das, S. K. Geospatial mapping of groundwater potential zones using multi-criteria decision-making AHP approach in a hardrock basaltic terrain in India. *Ecol. Indic.* (2021).
22. Magesh, N. S., Chandrasekar, N. & Soundranayagam, J. P. Delineation of groundwater potential zones in Theni district, Tamil Nadu, using remote sensing, GIS and MIF techniques. *Geosci. Front.* **3**(2), 189–196. <https://doi.org/10.1016/j.gsf.2011.10.007> (2012).
23. Senanayake, I. P., Dissanayake, D. M. D. O. K., Mayadunna, B. B. & Weerasekera, W. L. An approach to delineate groundwater recharge potential sites in Ambalantota, Sri Lanka using GIS techniques. *Geosci. Front.* **7**(1), 115–124. <https://doi.org/10.1016/j.gsf.2015.03.002> (2016).
24. Aju, C. D., Achu, A. L., Raicy, M. C. & Reghunath, R. Identification of suitable sites and structures for artificial groundwater recharge for sustainable water resources management in Vamanapuram River Basin, South India. *HydroResearch* **4**, 24–37. <https://doi.org/10.1016/j.hydres.2021.04.001> (2021).
25. Hasanuzzaman, M., Mandal, M. H., Hasnine, M. & Shit, P. K. Groundwater potential mapping using multi-criteria decision, bivariate statistic and machine learning algorithms: Evidence from Chota Nagpur Plateau, India. *Appl. Water Sci.* **12**(4), 1–16. <https://doi.org/10.1007/s13201-022-01584-9> (2022).
26. Hagos, Y. G. & Andualem, T. G. Geospatial and multi-criteria decision approach of groundwater potential zone identification in Cuma sub-basin, Southern Ethiopia. *Helijon* **7**(9), e07963. <https://doi.org/10.1016/j.helijon.2021.e07963> (2021).
27. Etikala, B., Golla, V., Li, P. & Renati, S. Deciphering groundwater potential zones using MIF technique and GIS: A study from Tirupati area, Chittoor District, Andhra Pradesh, India. *HydroResearch* **1**, 1–7. <https://doi.org/10.1016/j.hydres.2019.04.001> (2019).
28. Ghani, A. A. J. et al. Mapping groundwater potential zones in the Habawnah Basin of Southern Saudi Arabia: an AHP- and GIS-based approach. *Sustainability* **15**(13). <https://doi.org/10.3390/su151310075> (2023).
29. ASF Data Search Vertex. *EARTHDATA* (2024).
30. KIRS. *Kuwait Institute for Scientific Research* (1998).
31. Kwarteng, A. Y., Viswanathan, M. N., Al-Senayf, M. N. & Rashid, T. Formation of fresh ground-water lenses in northern Kuwait. *J. Arid Environ.* **46**(2), 137–155. <https://doi.org/10.1006/jare.2000.0666> (2000).
32. Albanai, J. A. Sea level rise projections for Failaka island in the state of Kuwait. *Trans. Marit Sci.* **9**(2), 236–247. <https://doi.org/10.7225/toms.v09.n02.008> (2020).

33. Al-Hurban, A., Albanai, J. A. & Elrawy, M. Comparison study on sedimentmorphological characteristics using Integrated Geo-Techniques: A case study of two Representative Areas in Kuwait. *J. Geogr. Inf. Syst.* **15**(01), 140–173. <https://doi.org/10.4236/jgis.2023.151009> (2023).
34. Meteoblue.
35. Mohammad, R. & Geographical information system based analysis of paleofluvial systems in the Kuwait region. *Univ. Pittsburgh3* (2008).
36. Al-Sulaimi, J., Khalaf, F. J. & Mukhopadhyay, A. Geomorphological analysis of paleo drainage systems and their environmental implications in the desert of Kuwait. *Environ. Geol.* **29**(1), 94–111. <https://doi.org/10.1007/s002540050108> (1997).
37. Al-Sulaimi, J. & Mukhopadhyay, A. An overview of the surface and near-surface geology, geomorphology and natural resources of Kuwait. *Earth Sci. Rev.* **50**(3), 227–267. [https://doi.org/10.1016/S0012-8252\(00\)0005-2](https://doi.org/10.1016/S0012-8252(00)0005-2) (2000).
38. El-Aziz, A., Abd El-Aal, K., Mohammed, J., Ali, A. A. & Ali, A. D. *The Geology of Kuwait* (2022).
39. Al-Rashed, M. F. & Sherif, M. M. Water resources in the GCC countries: An overview. *Water Resour. Manag.* **14**, 59–75 (2000).
40. Richards, G. & Moore, R. D. Suspended sediment dynamics in a steep, glacier-fed mountain stream, Place Creek, Canada. *Hydro. Process.* **17**(9), 1733–1753 (2003).
41. Sattar, B., Sayl, K. & Rashid, R. Modeling of spatially distributed sedimentation in Houran dam H-3. In *AIP Conference Proceedings* Vol. 3009 (2024).
42. Etikala, B., Golla, V., Li, P. & Renati, S. Deciphering groundwater potential zones using MIF technique and GIS: A study from Tirupati area, Chittoor District, Andhra Pradesh, India. *HydroResearch* (2019).
43. Ifediegwu, S. I. Assessment of groundwater potential zones using GIS and AHP techniques: A case study of the Lafia district, Nasarawa State, Nigeria. *Appl. Water Sci.* **12** 10. <https://doi.org/10.1007/s13201-021-01556-5> (2021).
44. Hagos, Y. G. & Andualem, T. G. Geospatial and multi-criteria decision approach of groundwater potential zone identification in Cuma sub-basin, Southern Ethiopia. *Helyyon* **7** (2021).
45. Dar, T., Rai, N. & Bhat, A. Delineation of potential groundwater recharge zones using analytical hierarchy process (AHP). *Geol. Ecol. Landsc.* **5**(4), 292–307. <https://doi.org/10.1080/24749508.2020.1726562> (2021).
46. Shebl, A. & Csámer, Á. Reappraisal of DEMs, Radar and optical datasets in lineaments extraction with emphasis on the spatial context. *Remote Sens. Appl. Soc. Environ.* **24**, 100617. <https://doi.org/10.1016/J.RSASE.2021.100617> (Nov. 2021).
47. Shebl, A., Atalla, M. A. & Csámer, Á. Vertical accuracy assessment of DEMs around Jabal Al-Shayeb area, Egypt. *Intercont. Geoinf. Days* **3**, 42–45 (2021).
48. Muneer, A. S., Sayl, K. N. & Kamal, A. H. Modeling of spatially distributed infiltration in the Iraqi Western Desert. *Appl. Geomatics.* **13**(3), 467–479. <https://doi.org/10.1007/s12518-021-00363-6> (2021).
49. Srivastava, S. K. *Delineation of Groundwater Potential Zone Through Geospatial Technique, Multi-Criteria Decision Analysis, And Analytical Hierarchy Procesc* 1–25 (2021).
50. Arulbalaji, P., Padmalal, D. & Sreelash, K. GIS and AHP techniques based Delineation of Groundwater potential zones: A case study from Southern Western Ghats, India. *Sci. Rep.* **9**(1), 1–17. <https://doi.org/10.1038/s41598-019-38567-x> (2019).
51. Hassan, A. et al. Assessment of flash flood risks in the desert cities: A case study on Sabah Al-Ahmad City, Kuwait. *J. Water Clim. Change* **jwc2024191** (2024).
52. Melese, T. & Belay, T. Groundwater potential zone mapping using Analytical Hierarchy process and GIS in Muga Watershed, Abay Basin, Ethiopia. *Glob. Chall.* <https://doi.org/10.1002/GCH2.202100068> (2021).
53. Magowe, M. & Carr, J. R. Relationship between lineaments and Ground Water occurrence in Western Botswana. *Groundwater* **37**(2), 282–286. <https://doi.org/10.1111/j.1745-6584.1999.tb00985.x> (1999).
54. Jari, A. et al. Use of GIS, remote sensing and analytical hierarchy process for groundwater potential assessment in an arid region—a case study. *Ecol. Eng. \& Environ. Technol.* (2022).
55. Saranya, T. & Saravanan, S. Groundwater potential zone mapping using analytical hierarchy process (AHP) and GIS for Kancheepuram District, Tamilnadu, India. *Model. Earth Syst. Environ.* **6**(2), 1105–1122. <https://doi.org/10.1007/s40808-020-0074-4-7> (2020).
56. Thapa, R., Gupta, S., Guin, S. & Kaur, H. Assessment of groundwater potential zones using multi-influencing factor (MIF) and GIS: A case study from Birbhum district, West Bengal. *Appl. Water Sci.* **7** (7), 4117–4131. <https://doi.org/10.1007/s13201-017-0571-z> (2017).
57. Rajaveni, S. P., Brindha, K. & Elango, L. Geological and geomorphological controls on groundwater occurrence in a hard rock region. *Appl. Water Sci.* **7**(3), 1377–1389. <https://doi.org/10.1007/s13201-015-0327-6> (2017).
58. Jaiswal, R. K., Mukherjee, S., Krishnamurthy, J. & Saxena, R. Role of remote sensing and GIS techniques for generation of groundwater prospect zones towards rural development—an approach, *Int. J. Remote Sens.* **24**(5), 993–1008. <https://doi.org/10.1080/01431160210144543> (2003).
59. Krishnamurthy, J. & Srinivas, G. Role of geological and geomorphological factors in ground water exploration: A study using IRS LISS data. *Int. J. Remote Sens.* **16**(14), 2595–2618 (1995).
60. Sayl, K. N., Sulaiman, S. O., Kamel, A. H. & Al-Ansari, N. Towards the generation of a spatial hydrological soil group map based on the radial basis network model and spectral reflectance band recognition. *Int. J. Des. Nat. Ecodyn.* **17**(5), 761–766 (2022).
61. Taloor, A. K., Manhas, D. S. & Kothiyari, G. C. Retrieval of land surface temperature, normalized difference moisture index, normalized difference water index of the Ravi basin using landsat data (2021).
62. Rulinda, C. M., Dilo, A., Bijk, W. & Stein, A. Characterising and quantifying vegetative drought in East Africa using fuzzy modelling and NDVI data. *J. Arid Environ.* **78**, 169–178. <https://doi.org/10.1016/j.jaridenv.2011.11.016> (2012).
63. Liu, Z., Yao, Z. & Wang, R. Assessing methods of identifying open water bodies using landsat 8 OLI imagery. *Environ. Earth Sci.* **75**, 1–13 (2016).
64. POWER Data Access Viewer., (2024).
65. Sensing, R. C. for H. Data Portal.
66. USGS - science for a changing world. Earth Explorer. *USGS - Science for a Changing World*.
67. USGS - science for a changing world. Welcome to the WorldView-1/2/3/4 information area. *ESA Earth Online* (2021).
68. Gorelick, N. et al. Google Earth Engine: Planetary-scale geospatial analysis for everyone. *Remote Sens. Environ.* **202**, 18–27. <https://doi.org/10.1016/j.rse.2017.06.031> (2017).
69. Yang, M., Wang, H., Hu, K., Yin, G. & Wei, Z. An inception–attention-module-based network for classifying underwater images from others. *IEEE J. Ocean. Eng.* **47**(3), 704–717 (2022).
70. Xu, J., Zhou, G., Su, S., Cao, Q. & Tian, Z. The development of a rigorous model for bathymetric mapping from multispectral satellite-images. *Remote Sens.* **14**(10), 2495 (2022).
71. Zhou, G. & Liu, X. Orthorectification model for extra-length linear array imagery. *IEEE Trans. Geosci. Remote Sens.* **60**, 1–10 (2022).
72. Zhou, G. et al. Orthorectification of fisheye image under equidistant projection model. *Remote Sens.* **14**(17), 4175 (2022).
73. Sameer, Y. M., Abed, A. N. & Sayl, K. N. Highway route selection using GIS and analytical hierarchy process case study Ramadi Heet rural highway. *J. Phys.* **1973**(1), 12060 (2021).
74. Viera, A. J. & Garrett, J. M. and others, Understanding interobserver agreement: The kappa statistic, *Fam. Med.* **37**(5), 360–363 (2005).

Acknowledgements

Thanks to ESA for providing Sentinel 2 data. Ali Shebl is funded by Stipendium Hungaricum scholarship under the joint executive program between Hungary and Egypt. The research was financed by the NKFI K138079. The research was fully funded by University North, Croatia, Scientific project UNIN-TEH-24-1-15 Detection of underground infrastructure (2024).

Author contributions

MA: Writing- review & editing, Writing- original draft, Visualization, Validation, Software, Methodology, Investigation, Formal analysis, Data curation, Supervision, Resources, visualization, Project administration, Conceptualization. AS: Writing- review & editing, Supervision, Funding acquisition, visualization, Conceptualization. NK: Writing- review & editing, visualization, BD: Linguistic review & editing. WA: Writing- review & editing, Writing- original draft, Visualization, Validation, Methodology, Supervision, visualization, Project administration, Conceptualization. All authors have read and agreed to the published version of the manuscript.

Declarations

Competing interests

The authors declare no competing interests.

Additional information

Supplementary Information The online version contains supplementary material available at <https://doi.org/10.1038/s41598-024-76989-4>.

Correspondence and requests for materials should be addressed to A.S. or N.K.

Reprints and permissions information is available at www.nature.com/reprints.

Publisher's note Springer Nature remains neutral with regard to jurisdictional claims in published maps and institutional affiliations.

Open Access This article is licensed under a Creative Commons Attribution-NonCommercial-NoDerivatives 4.0 International License, which permits any non-commercial use, sharing, distribution and reproduction in any medium or format, as long as you give appropriate credit to the original author(s) and the source, provide a link to the Creative Commons licence, and indicate if you modified the licensed material. You do not have permission under this licence to share adapted material derived from this article or parts of it. The images or other third party material in this article are included in the article's Creative Commons licence, unless indicated otherwise in a credit line to the material. If material is not included in the article's Creative Commons licence and your intended use is not permitted by statutory regulation or exceeds the permitted use, you will need to obtain permission directly from the copyright holder. To view a copy of this licence, visit <http://creativecommons.org/licenses/by-nc-nd/4.0/>.

© The Author(s) 2024